Atmos. Meas. Tech. Discuss., 1, 321–374, 2008
www.atmos-meas-tech-discuss.net/1/321/2008/
© Author(s) 2008. This work is distributed under
the Creative Commons Attribution 3.0 License.

Atmospheric Measurement Techniques Discussions

Atmospheric Measurement Techniques Discussions is the access reviewed discussion forum of *Atmospheric Measurement Techniques*

Experimental characterization of the COndensation PArticle counting System for high altitude aircraft-borne application

R. Weigel[1,*], M. Hermann[2], J. Curtius[3,4], C. Voigt[5], S. Walter[1], T. Böttger[1], B. Lepukhov[6], G. Belyaev[6], and S. Borrmann[1,3]

[1]Max Planck Institute for Chemistry, Particle Chemistry Department, Mainz, Germany
[2]Leibniz Institute for Tropospheric Research, Leipzig, Germany
[3]Institute for Atmospheric Physics, Johannes Gutenberg-University, Mainz, Germany
[4]Inst. for Atmosphere and Environment, Johann Wolfgang Goethe Univ., Frankfurt, Germany
[5]Deutsches Zentrum fuer Luft- und Raumfahrt, Institut für Physik der Atmosphäre, Oberpfaffenhofen, Germany
[6]Myasishchev Design Bureau, Moscow, Russia
[*]now at: Lab. de Météorologie Physique, Univ. Blaise Pascal, Clermont-Ferrand, France

Received: 17 September 2008 – Accepted: 31 October 2008 – Published: 28 November 2008

Correspondence to: R. Weigel (r.weigel@opgc.univ-bpclermont.fr)

Published by Copernicus Publications on behalf of the European Geosciences Union.

Abstract

This study aims at a detailed characterization of an ultra-fine aerosol particle counting system for operation on board the Russian high altitude research aircraft M-55 "Geophysica" (maximum ceiling of 21 km). The **CO**ndensation **PA**rticle counting **S**ystems (COPAS) consists of an aerosol inlet and two dual-channel continuous flow Condensation Particle Counters (CPCs).

The aerosol inlet, adapted for COPAS measurements on board the M-55 "Geophysica", is described concerning aspiration, transmission, and transport losses. The counting efficiencies of the CPCs using the chlorofluorocarbon FC-43 as the working fluid are studied experimentally at two pressure conditions, 300 hPa and 70 hPa. Three COPAS channels are operated with different temperature differences between the saturator and the condenser block yielding smallest detectable particle sizes (d_{p50} – as 50% detection "cut off" diameters) of 6 nm, 11 nm, and 15 nm, respectively, at ambient pressure of 70 hPa. The fourth COPAS channel is operated with an aerosol heating line (250°C) for a determination of the non-volatile number of particles. The heating line is experimentally proven to volatilize pure H_2SO_4-H_2O particles for a particle diameter (d_p) range of 11 nm<d_p<200 nm.

Additionally this study includes investigation to exclude auto-nucleation of the working fluid inside the CPCs. An instrumental inter-comparison (cross-correlation) has been performed for several measurement flights and mission flights in the Arctic and the Tropics are discussed. Finally, COPAS measurements are used for an aircraft plume crossing analysis.

1 Introduction

High altitude in-situ measurements of fine aerosol particles (d_p<100 nm) are essential for studies concerning the atmospheric radiative budget, stratospheric chemistry, polar stratospheric cloud (PSC) microphysics, as well as for comparisons with ground

AMTD

1, 321–374, 2008

based or satellite borne remote sensors. Aerosol particles in the stratosphere play a clearly different role in the atmospheric physico-chemical context than tropospheric particles. The stratospheric environment is, in a dynamical sense, relatively undisturbed compared to the troposphere. The time scale for particle and gas interactions, photo-chemical processes or physico-chemical transformation under quasi-undisturbed stratospheric conditions is larger, i.e. weeks and months, compared to equivalent processes in the troposphere which last from hours to days (SPARC, 2006).

Seminal work on the subject of stratospheric aerosol was performed by Junge and co-workers leading to the discovery of an Earth spanning stratospheric aerosol layer and to the investigation of the stratospheric aerosols content (Junge et al., 1961; Junge and Manson, 1961; Junge, 1961). Until today numerous studies were performed to investigate the origin of aerosol particles at stratospheric altitudes, their stratospheric lifetimes as well as their physical behavior, e.g. scattering of solar radiation, and therefore their possible effects on the global radiation budget (see e.g., SPARC, 2006 and references therein). Due to the fact that stratospheric aerosol particles scatter solar radiation, these particles exert a significant influence on the stratosphere's radiation budget, and on the Earth's planetary albedo (Hamill et al., 1997 and references therein). Another important objective of investigations is to determine the quantitative and qualitative contribution of aerosol particles to chemical transformation processes in the stratosphere. The particles provide the essential surfaces for several chemical reactions (Prather and Rodriguez, 1988; Peter, 1997). For example, stratospheric aerosol particles play a significant role in heterogeneous processes forming reactive chemical species which are known to participate in ozone depletion (Peter, 1997; Borrmann et al., 1997; Voigt et al., 2000, 2005).

Episodic explosive volcanic eruptions (e.g., El Chichón in Mexico, 1982, or Mount Pinatubo on the island of Luzon, Philippines, 1991) can contribute significantly to the stratospheric aerosol mass (e.g., up to 30 Mt of additional aerosol material by the 1991 eruption of Mount Pinatubo, WMO, 1995) with significant influence on the Earth's climate over a period of years after such an eruption (e.g., Hofmann and Solomon, 1989;

CC BY

Wilson et al., 1993; Jònsson et al., 1996; Borrmann et al., 2000; Deshler et al., 2003). Within five to seven years the stratospheric pre-eruptive condition is reached again (Deshler et al., 2003) due to particle sink processes such as sedimentation into the lowermost stratosphere (LS) and dynamic exchange with the upper troposphere (UT) (Holton et al., 1995). Additionally, subsiding air masses inside the polar winter vortex remove particles from the stratosphere (Holton et al., 1995; Curtius et al., 2005). Nevertheless, so far the processes that lead to the maintenance of a quasi constant background concentration of stratospheric aerosol in periods of volcanic quiescence, as observed e.g., by Ansmann et al. (1996), are not fully understood and are the subject of numerous other studies (e.g. Brock et al., 1995; Murphy et al., 1998; Deshler et al., 2003; Notholt et al., 2003; Murphy et al., 2007; etc.). Recent interest in the physicochemical properties and spatial/temporal evolution of the stratospheric aerosol layer was sparked by the suggestion to artificially enhance this layer to achieve increased shortwave reflection for partially compensating the global warming (Crutzen, 2006; Cicerone, 2006; Bengtsson, 2006).

A major fraction of the stratospheric aerosol is assumed to consist of ~75-weight-percent solution of sulfuric acid and water (H_2SO_4/H_2O) (Rosen, 1971; Arnold et al., 1998; Murphy et al., 2007). Besides H_2SO_4-H_2O particles, also refractory compounds are found in stratospheric particles, such as soot (or other refractory carbonaceous material), meteoric material and volcanic ashes (Turco et al., 1982; Murphy et al., 1998; Cziczo, 2001; Curtius et al., 2005; Murphy et al., 2007). Particularly the refractory material might have a significant impact on various processes such as PSC activation in the polar winter vortex (Peter, 1997; Murphy et al., 1998; Curtius et al., 2005; Voigt et al., 2005; Murphy et al., 2007).

Since 2002, the University of Mainz and the Max Planck Institute for Chemistry in Mainz (Germany) developed and operated two separate units of aircraft-borne dual-channel condensation particle counters (CPCs), the **CO**ndensation **PA**rticle counting **S**ystems (COPAS), on board the high altitude research aircraft M-55 “Geophysica” (http://emz-m.ru/M55-e.htm). The terminus of two dual-channel CPCs is used in this

CC BY

study to refer to two independent units, each containing two coupled CPCs. For technical reason two CPCs are thermally coupled in each of the two COPAS units by a common heat sink. Additionally, the two COPAS units are operated with one aerosol inlet, each. Therefore, the altogether four COPAS channels can not be considered to be independent CPCs.

In recent years, several measurement campaigns with participation of COPAS allowed for intensive studies of ultra-fine particles in the UT/LS. More than 11 years after the last massive volcanic eruption of Mount Pinatubo these campaigns provided the opportunity to investigate the stratospheric aerosol under undisturbed conditions using aircraft-borne measurements. Therefore the COPAS CPCs were operated in the Arctic, the mid-latitude and the tropical UT/LS.

The COPAS instrument was originally based on a CPC design developed by the University of Denver (USA) for measurements on board the NASA ER-2 (Wilson et al., 1983). However, the operation on board the M-55 "Geophysica" – especially under the environmental conditions in the tropics – required major modifications of the instrumental setup and the data management (cf. Sect. 2). Two almost identical versions of the dual-channel COPAS instruments have been built and operated simultaneously on board the M-55 "Geophysica". The two COPAS instrument units provide altogether four CPC channels. One goal is given by the fact that two COPAS units with two channels each were implemented at different positions on board of the M-55 "Geophysica". The obvious drawback of thus having to provide two separate inlets, thermal control systems, power supplies etc. turned out to be advantageous for example in case of electrical failures. Also the independent measurements of such disjoint units provide additional credibility to the data. The information from these four CPC channels is used to obtain a) the total number concentration of particles with diameters larger that 11 nm, b) the number concentration of ultra-fine particles (with diameters 6 nm$<d_p<$15 nm) by operating two CPCs with different temperatures of the saturator and the condenser, and c) the concentration of stratospheric aerosol particles with refractory cores larger that 11 nm diameter by using an aerosol heating line upstream of one COPAS channel.

AMTD
1, 321–374, 2008

This study provides the first detailed description as well as a comprehensive characterization of the CPCs counting efficiency and other critical instrument parameters at the relevant atmospheric conditions. For several CPC models (e.g., by TSI Inc.) there is information on their performance at reduced pressures available in the literature based on experimental as well as theoretical work (Heintzenberg and Ogren, 1985; Dreiling and Jaenicke, 1988; Saros et al., 1996; Zhang and Liu, 1990; Cofer et al., 1998; Noone and Hansson, 1990; Zhang and Liu, 1991; Herrmann and Wiedensohler, 2001, and Herrmann et al., 2005). A detailed description of both, the instrumental development and the instrument performance of those CPCs at reduced operating pressure, is given by Hermann and Wiedensohler (2001) who also provided a description of a low-pressure calibration setup. This setup allows for generating different aerosol particles of specific size in sufficient quantities and for operating at a pressure range from 1000 hPa down to 50 hPa. All experimental characterizations presented in this study concerning the pressure dependent counting efficiencies of the COPAS CPCs were carried out at the Leibniz Institute for Tropospheric Research, Leipzig, Germany. The characterization included also coincidence studies, as the coincidence effect is strongly dependent on the individual CPC design. Furthermore, the possibility of autonucleation – the formation of new particles from the supersaturated working liquid in absence of ambient aerosol particles inside the CPC – was analyzed. To correct the measured particle concentrations for inlet losses, the aerosol inlet system, which is exclusively used for the COPAS measurements on board the M-55 "Geophysica", is described taking into account aspiration, transmission, and transport.

Also subject of the experiments was to characterize the vaporizing properties of the aerosol pre-heating device. Previous work on volatilization properties of aerosols, particularly oriented to the stratospheric H_2SO_4-H_2O aerosol component, has been performed e.g. by Rosen (1971); Deshler et al. (1993) and Brock et al. (1995).

Furthermore, a correlation of the different COPAS CPC channels for six measurement flights was analysed, when the CPCs were operated at identical temperature settings and therefore identical threshold diameters. As another example two research

CC BY

flights were chosen, one of measurements in the Arctic and one from studies in tropical regions, to demonstrate the instrumental performance and possible outcome as well as the limits of the COPAS operation, particularly with respect to the flight altitude. Finally, two crossings of the M-55 "Geophysica's" own exhaust at altitudes of 16–18 km were used to estimate the particle emission index for different aerosol size classes emitted by the M-55 "Geophysica" as an example for immediate use of COPAS data.

2 Details of the instrumental design

The COPAS CPCs are thermo-diffusion-type counters which are usually operated with butanol (C_4H_9OH) or FluorInert FC-43 ($(C_4F_9)_3N$), a commercially available fluorocarbon, as working fluids. The process of thermo-diffusion in the condenser volume leads to supersaturation followed by particle growth up to sizes at which the particles are sufficiently large to be optically detected. To allow for continuous sampling with a frequency ≤1 Hz and precise measurements at particle concentrations <100 cm^{-3}, this working principle is used for COPAS instead of expansion-type CPCs (e.g. Scholz, 1931 and 1932; Junge, 1935 and 1961; Jaenicke and Kanter, 1976; Wagner, 1982; Szymanski and Wagner, 1983; Yang, 1999; Kürten et al., 2005).

Commercially available CPCs usually have threshold diameters – which is the smallest diameter d_{p50} at which 50% of the existing particles are still detected – between 2.5 and 20 nm. CPCs used on research aircraft in the past usually had threshold diameters of 3–10 nm (e.g. Wilson et al., 1983; Dreiling and Jaenicke, 1988; Brock et al., 1995; Hermann and Wiedensohler, 2001; Minikin et al., 2003). For laboratory applications and ground-based field measurements it was demonstrated that particles smaller than 1.2 nm can be detected with CPCs (Sgro and de la Mora, 2004; Kulmala 2007; Sipilä et al., 2008). Reviews on the general designs and the development of different types of CPCs are available from McMurry (2000) and Spurny (2000).

The COPAS operation principle with actively controlled volumetric sample air flow is shown in Fig. 1. The dual channel COPAS is equipped with one aerosol inlet. Thus, the

CC BY

total incoming airflow is split into two CPC flows (cf. general COPAS unit flow scheme box in Fig. 1). In each CPC channel, the incoming airflow is split again into two subflows. The major part of the flow (~90%) is cleaned from aerosol particles by a total aerosol filter. Subsequently, the cleaned air becomes saturated with the vapor of the working liquid in the saturator chamber which is maintained at a constant temperature (COPAS-I: both channels 32°C; COPAS-II: 24°C and 40°C for channel one and two, respectively). The remaining fraction of the incoming air (~10%) is the sample flow which carries the aerosol particles. The minor flow passes a capillary with a nozzle-shaped tip. At the exit of this capillary the two subflows – the sample flow and the particle-free, saturated air – are merged again. The saturated airflow now acts as a sheath flow which focuses the sample flow into the condenser and thus helps to avoid particle losses due to turbulences, diffusion, and thermophoretic effects (Wilson et al., 1983). In the condenser the total air flow is cooled to temperatures of 2°C (COPAS-I) and 7°C (COPAS-II) leading to a supersaturation of the working fluid vapor. This supersaturation drives the growth of the aerosol particles to sizes that are detectable by a suitable photo-optical sensor (equipped with a 50 mW laser diode, wave length λ=780 nm) which is comparable to the detector of the CPC TSI model 3760 (cf. TSI Incorporated, 2002).

The total flow rates of the COPAS units are monitored by use of differential pressure sensors at the sample flow capillary and the common exhaust line for both CPCs. The automated flow regulation (with 10 Hz integration loop frequency) of each COPAS instrument controls the air pump frequency (and therefore the flow rate of both CPCs of one COPAS) according to settings which can be described by the linear relation $y=a\cdot x+b$ of total standard volume flow rate (y) in $cm^3\ min^{-1}$ as a function of ambient pressure (x) in hPa with the parameters for COPAS-I: a=2.09, b=40.60 and COPAS-II: a=2.23, b=36.56. The automated flow regulation generally works within an accuracy range of ±15%. However, if ascent and descent rates of the airborne platform significantly exceed 10 ms^{-1} the differential pressure measurement shows disturbances, probably caused by turbulent flow conditions within the flow measurement

AMTD
1, 321–374, 2008

volume. Irregular flow measurements have direct influence on the air flow regulation and therefore on the instrumental performance (cf. Sect. 8).

The differential pressure measurement requires a calibration related to the volume flow rate, which is dependent on the pressure conditions. A bubble flow meter was used to calibrate the flow rate derived from the changes of measured differential pressure of each COPAS channel in the pressure range of 1000–50 hPa (Weigel, 2005).

2.1 Adaptation to airborne operation

The COPAS CPCs – intended for aircraft-based applications at altitudes up to 21 km – have to fulfill special instrumental requirements such as operating pressures down to 50 hPa and temperature conditions from +50°C (at an airfield's runway) down to −90°C in the UT/LS and changes between these extremes within 20 min. The instruments on board the M-55 "Geophysica" are not mounted inside a pressurized, air-conditioned cabin and thus subjected to such changes in ambient conditions. Important properties of the COPAS instruments are:

- The saturator of each COPAS channel is equipped with an active heating device. Thus the saturator temperature is maintained at its set-points within ±0.5°C during a complete flight (in the Arctic as well as in tropical regions).
- FluorInert (FC-43) is preferably used as the working liquid instead of butanol. In particular, for CPC applications at high altitudes with pressure conditions below 400 hPa the use of FC-43 is favored due to its better performance (Hermann et al., 2005) (cf. Sect. 8) and has also been used on the NASA ER-2 (J. C. Wilson, University of Denver, Colorado, USA, personal communications, 2003).
- Peltier elements are used for the cooling of the condenser, with their warm sides being cooled by a low viscosity silicone oil circuit. Because of the low pressure conditions at high flight altitudes, the use of conventional air-cooled heat sinks proved not to be sufficient to prevent overheating of the Peltier elements and

CC BY

several different designs of such cooling systems failed during M-55 "Geophysica" flights. A custom-designed oil circuit is running through the shaft of the inlet probe, where the oil is efficiently cooled (Fig. 2). Minimum oil temperatures of $<-37^{\circ}$C are reached during flight at ambient temperatures of $<-70^{\circ}$C (UCSE – Unified Communications for Systems Engineer – recorded and processed by the M-55 "Geophysica" operator, Myasishchev Design Bureau, Moscow, Russia). For such low oil temperatures the Peltier elements are only used for adjusting the temperature to a certain set point while they can be operated in both modes, cooling and heating. This setup, together with thermal isolation allows for maintaining the COPAS condenser temperature within $\pm 0.5^{\circ}$C as was determined experimentally during the flights.

- The air flow through the COPAS unit is regulated by a frequency-controlled air pump (Brey G12/02-8) according to ambient pressure variation with 10 Hz integration loop frequency at standard temperature and pressure (STP).
- The data acquisition and control of COPAS is achieved by custom-made electronics. Data are typically recorded with 1 Hz frequency on flash memory (PCMCIA card).

2.2 The inlet probe

The inlet probe for measurements on board the M-55 "Geophysica" consists of three parts, the base plate, the shaft, and the inlet head. Figure 3 shows a schematic drawing of the different parts and photographic images of the implementation.

For the COPAS measurements on board the M-55 "Geophysica" a diffuser-type, non-shrouded inlet with sharp-edged inlet lips was used (with diffuser cone half-angle of 2.9°). This inlet is a custom-made reproduction in accordance to the original inlet design which was used on board the NASA ER-2 and which is described in detail by Wilson et al. (1992). For the M-55 "Geophysica" additional modifications were necessary in particular with respect to the angle of attack and the airflow around the aircraft

AMTD
1, 321–374, 2008

hull.

The shaft length of 300 mm insures an aerosol probing well outside the boundary layer of the aircraft M-55 “Geophysica” (Myasishchev Design Bureau, Moscow, Russia, M-55 Aircraft Technical Design Specification documents). Beside the aerosol sampling line and the exhaust tube the shaft contains the oil cooling circuit (cf. Sect. 2.1).

2.3 The condenser cooling oil circuit

The graphics in Fig. 2 show the measured oil temperature during a flight in tropical region (12 February 2005, TROCCINOX mission, Araçatuba, Brazil) as an example for extreme ambient temperature conditions influencing the COPAS measurement performance. The ambient temperatures as well as the oil temperatures are shown as a function of flight altitude. From the temperature profiles it becomes obvious that high ambient temperatures on the ground caused oil temperatures of up to 33°C. The oil temperature remained above 10°C until flight altitudes of 12 km. At 12 km altitude an oil temperatures of 10°C is reached for which the condenser temperature is in the range of given settings as also for the rest of this flight.

For oil temperatures above 10°C the condenser temperatures are out of range and according measurement data have to be discarded from further analysis (cf. Sect. 8). So, for future missions, in particular at regions of high air temperature a cooling of the whole COPAS system prior to a flight is going to be considered.

3 Determination of COPAS sampling characteristics

The performance of an aerosol inlet system can be described by the inlet particle sampling efficiency (aspiration and transmission) and the transport efficiency through the sampling lines to the instruments (Baron and Willeke, 2001). The aspiration is related to the fraction of the ambient particles which enter the aerosol inlet, while the transmission efficiency denotes the particle fraction that passes through the inlet. The

AMTD
1, 321–374, 2008

transport efficiency is determined by the particle losses in the sampling line between the inlet and the instrument and describes the fraction of particles that are able to reach the detection chamber. The following three sections describe the sampling efficiency of the COPAS aerosol inlet and the aerosol sampling line transport efficiency.

3.1 Aspiration efficiency of the COPAS aerosol inlet

For representative measurements an aerosol probe must sample well outside of the aircraft boundary layer and outside of zones of shadow or enhancement for particles caused by the aircraft hull. These conditions are met for both COPAS positions on board the M-55 "Geophysica".

For isoaxial sampling the specific angle of attack of an aircraft has to be counter-vailed by alignment of the aerosol inlet. Assuming a mean angle of attack of 7° for the M-55 "Geophysica" the alignment of the COPAS aerosol inlet generally meets the requirement of isoaxial sampling. Discrepancies from the isoaxial alignment of the COPAS aerosol inlet which are in the range of ±1.5° can be neglected for sub-micrometer particle sampling since aerosol losses particularly are a function of particle inertia. Particle loss based on anisoaxial sampling gets significant for larger particles and droplets (Herrmann et al., 2001).

To evaluate the isokinetic property of the COPAS aerosol inlet 2-D CFD modeling studies with FLUENT were performed by Walter (2004). For the calculations compressible gas properties were assumed considering the maximum flight speed of the M-55 "Geophysica" of up to Mach 0.7 (Myasishchev Design Bureau, 2002).

Figure 4 shows CFD model results obtained by Walter (2004) for the flow velocity around the inlet head for a mean aircraft cruising velocity of 170 ms^{-1}. From this graphic it can be seen that the air velocity is already decelerated down to 140 ms^{-1} at the entrance of the inlet head indicating that the sampling with the COPAS aerosol inlet is slightly sub-isokinetic (ratio of the free air velocity and the flow velocity inside the aerosol inlet R=1.2).

Further deceleration of the air flow inside the inlet head yields a flow velocity of

AMTD
1, 321–374, 2008

about 60 ms^{-1} at the point where the inner probe is located (Walter, 2004). A pressure dependent total standard volume sample flow rate between approximately 2.2 l min^{-1} (STP) (at 1000 hPa) and 0.15 l min^{-1} (STP) (≈3.0 l min^{-1} at 50 hPa) for both COPAS CPCs (cf. Sect. 2) enters the inner probe which has an inner diameter of 1.35 mm. Thus, considering the flow rate under ambient pressure conditions, this yields an air flow velocity at the probe entrance of approximately 35 m s^{-1}. With the result of the inlet head air velocity of 60 m s^{-1} again a sub-isokinetic sampling can be concluded for the probe diffuser (R=1.7).

For calculation of the aspiration efficiency E_a the equations from Hangal and Willeke (1990) are used for ambient pressure of 50 hPa, considering that any anisokinetic effect has the largest impact on particle losses at lowest pressure conditions. Calculations were made related to the probe head entrance assuming R=1.2 and for the probe inlet with R=1.7 as the ratios of air flow velocities. The sampling conditions are sub-isokinetic at the inlet head entrance as well as at the probe itself which becomes significant for particle sizes well above d_p=500 nm. However, as the particle number concentration in the UT/LS is strongly dominated by the sub-micrometer particles of d_p<500 nm (Deshler et al., 2003; Thomas et al., 2002) the results indicate that here, at UT/LS altitudes, the obtained aspiration efficiency of the inlet has negligible impact on the measurement with COPAS.

3.2 Transmission efficiency

The COPAS aerosol inlet has sharp-edged inlet lips and an inlet cone half-angle of 2.9°, which is small enough to prevent flow separation inside the diffuser.

Hermann et al. (2001) provide results of wind tunnel experiments with an aircraft-borne aerosol inlet. They showed that in the range of interest the transmission is independent from the Reynolds-number and that the transmission efficiency of their inlet decreased for particles larger than 200 nm, reaching zero at about 3 μm. Such wind tunnel experiments have not been performed for the COPAS aerosol inlet. We as-

CC BY

sume that the findings for the inlet by Hermann et al. (2001) can be transferred to our inlet as it represents a very similar non-shrouded diffuser-type inlet head with a rather sharp-edged inlet entrance. Although the sampling inside the inlet head of their system is realized by a backward facing probe, in contrast to the COPAS-inlet, Hermann et al. (2001) showed transmission efficiencies well above 75% for submicron particles. Considering that the particle number concentration in the UT/LS is relatively small for particles with diameters d_p>1 μm (Deshler et al., 2003; Thomas et al., 2002) the transmission of the COPAS aerosol inlet can be estimated to be about 1 for d_p<500 nm and better than 0.75 for the sub-micron particle size range of 500 nm<d_p<1 μm.

3.3 Transport efficiency

The transport through the COPAS aerosol tubes causes particle losses due to diffusion, particularly in the size range 1 nm<d_p<100 nm. For the diffusional loss mechanism, the particle fraction that penetrates the aerosol lines can be calculated using empirical equations given by Baron and Willeke (2001) and Hinds (1999).

In the M-55 "Geophysica" system aerosol particles first have to pass a distance of 900 mm inside a stainless steal tube with inner diameter of 4 mm from the probe entrance to the COPAS counters (aerosol residence time inside these tubes ranges between 0.2 and 0.9 s). For the calculations a temperature T=223.2 K and a pressure range of 600 hPa–70 hPa were assumed for the particle size range 1 nm<d_p<1 μm. For the calculations the volume flow rate was varied between 1.64×10^{-5} $m^3\,s^{-1}$ and 3.94×10^{-6} $m^3\,s^{-1}$.

For the heated COPAS channel only, the aerosol particles have to pass an additional tube distance with a total length of 1300 mm of variable inner tube diameter (from 4 mm for a length of 150 mm, to 10 mm for a length of 1000 mm, to 4 mm for a length of 150 mm). The stainless steel tube is bent twice, a 180° bend with bend diameter of 300 mm and a 90° bend with a bend diameter of 100 mm. Furthermore, a heating temperature of 523.2 K must be considered in the calculations.

CC BY

In Table 1 the results of the diffusional loss calculations are summarized separately for the regular (non-heated) and the preheated aerosol sampling line as function of operating pressure and particle size. Apparently the measured numbers of aerosol particles with sizes smaller than 10 nm roughly represent the ambient particle number within a factor of two. The count results from the heated channel are interpreted to show significant features if the difference in particle number between heated and unheated channel with 10 nm cut off size is larger than 10%.

A general problem arises from the fact that any size dependent correction of the measured particle number concentration related to the particle losses and the counting efficiency of COPAS requires the knowledge of the initial aerosol size distribution. Corrections for the particle number concentration are impossible without that knowledge. But for the measurement of the ultra-fine nucleation-mode particles, a correction is feasible.

For the field measurements, the COPAS CPCs are operated with different lower threshold diameters and by subtracting the readings of two COPAS CPCs, for example the two channels of COPAS-II, with d_{p50}≈6 nm ($\Rightarrow n_6$) and with d_{p50}≈15 nm ($\Rightarrow n_{15}$), the number concentration of particles in the size range between 6 and 15 nm (n_{6-15}) can be determined. According to the empirical equations by Baron and Willeke (2001) and Hinds (1999) particle losses can be calculated and averaged as a mean particle loss for the complete fraction of particles between 6 and 15 nm (Table 3). The particle number concentration n_{6-15} has to be corrected with the calculated correction factor κ_L dependent on the pressure condition of <150 hPa, 150–300 hPa, and >300 hPa, respectively.

4 Determination of COPAS detection and counting characteristics

The ratio between the detected (n_{det}) and the real (n_{real}) particle number concentration at a given particle size is defined as the counting efficiency $\eta(d_p)$ of a particle counter. From the counting efficiency at $\eta(d_p)$=50% the "smallest" detectable particle size (cut-

CC BY

off or threshold diameters), denoted as d_{p50}, can be determined in dependency on the supersaturation which can be adjusted within a certain range by changing the temperature difference ΔT between the saturator (T_{Sat}) and the condenser (T_{Cond}).

An additional important parameter for CPC characterization is the pressure dependent maximum asymptotic counting efficiency. This parameter describes the plateau value of the counting efficiency for larger aerosol particles. Hermann and Wiedensohler (2001) showed for the Model 7610 (TSI Inc.), operated with butanol, that the maximum asymptotic counting efficiency decreases significantly with decreasing pressure for pressures below 300 hPa. However, Hermann et al. (2005) showed an opposite behavior for FC-43 used as working fluid inside the same CPC type.

Silver (Ag) particles were used in this study to determine the counting efficiencies of the COPAS CPCs, as Ag particles can be produced more easily in sufficiently high number concentration for particle diameters of a few nanometers (<4 nm). Silver particles can be generated in nearly spherical shape, they are physically stable as well as inert with respect to chemical reactions.

The calibration set-up used for the COPAS characterization is described in detail by Hermann and Wiedensohler (2001) and Hermann et al. (2005). The calibration aerosol is charged by a neutralizer (^{241}Am source) and a monodisperse fraction is selected by a Differential Mobility Analyzer (DMA, Vienna-type, short) (Hermann and Wiedensohler, 2001). The COPAS CPC is positioned parallel to an Aerosol Electrometer (AE) used as the reference counter. In an Aerosol Electrometer the aerosol particles are sampled on a total particle filter which is placed inside a Faraday cup. Charged particles deposited on the filter are detected by measuring the displacement current that results between the grounded housing and the Faraday cup (for details cf. TSI Incorporated, 2003 and references therein). For particles with d_p<20 nm the displacement current is directly proportional to the particle number concentration, assuming that each particle of this size carries only single electrical charge. For larger particles, the effect of multiple charges has to be considered. For the relevant particle size range within this study (4 nm<d_p<35 nm) uncertainties stay below 5%. Both instruments are op-

CC BY

erated inside the low pressure part of the calibration set-up at pressures from 1000 to 50 hPa depending on instruments and flow rates used. For the COPAS characterization pressures from 70 hPa to 300 hPa were covered. The operating temperatures of the COPAS-I were T_{Sat}=32°C and T_{Cond}=2°C ($\Rightarrow \Delta T$=30°C), common for both channels. The channels 1 and 2 of COPAS-II were operated with T_{Sat}=24°C and T_{Cond}=7°C and T_{Sat}=40°C and T_{Cond}=7°C ($\Rightarrow \Delta T_1$=17°C and ΔT_2=33°C), respectively.

Figure 5a–d shows the results of the characterization of both COPAS CPCs for a particle sizes range of 5 nm<d_p<35 nm for two pressure conditions, 70 hPa and 300 hPa. The curves represent linear interpolations between two consecutive values. The error bars on the x-axis represent theoretical values of the bandwidth of the DMA transfer function. The error bars on the y-axis display the standard deviation from the measurement mean. For each particle diameter and both pressure conditions four measurement points were recorded.

Table 3 summarizes the resulting d_{p50} for the COPAS channels for two pressure conditions. For the field measurements, the two channels of COPAS-I, with very similar cut-offs at d_{p50}≈11 nm, are used to study the refractory fraction of the total particle number concentration. The difference in the efficiency characteristic between the two COPAS-I channels results from the mounted (but not heated) heating line at channel 1 (see Fig. 5a). Two effects can be observed due to the elongated aerosol tube – a shift of d_{p50} to larger sizes and a decreased maximum asymptotic counting efficiency for channel 1 (7–12% lower compared to channel 2). These effects are caused by additional particle losses. Thus, in particular the decreased maximum asymptotic counting efficiency yields a correction of the heated channel measurements of generally not more than 10%.

The channels of COPAS-II have significantly different cut-offs, d_{p50}≈12 nm (at 70 hPa) for channel 1 (with increasing atmospheric pressure up to d_{p50}≈19 nm (at 300 hPa) and d_{p50}≈6 nm for channel 2, nearly independent of pressure. For sake of simplicity, also a pressure independent mean cut-off of d_{p50}=15 nm for channel 1 is used generally. The difference between the two COPAS II channels is used to inves-

AMTD
1, 321–374, 2008

tigate the occurrence or absence of freshly nucleated aerosol particles in the atmosphere.

The accuracy of the COPAS measurements within the particle size range 6 nm<d_p<35 nm was determined from the characterisation experiments. For both pressure conditions, 70 hPa and 300 hPa, the repeated measurements yield values of mean standard deviation for each COPAS channel which are listed in Table 3. Generally, the variability ranges between ±9% and ±3%. The values of ±14.2% and ±11.6% for the COPAS-I calibration at 70 hPa are regarded as outliers due to a relatively low number concentration of generated calibration aerosol. Unfortunately, these measurements could not be repeated with higher particle concentration. However, a general collective accuracy of the COPAS instruments over the particle size range 6 nm<d_p<1 μm is estimated to be within ±10%. This value was obtained from the previous experimental and analytical results and from comparison with other laboratory CPCs using the same threshold limits as COPAS.

5 Coincidence and auto-nucleation

"Coincidence" describes the classification of two or more particles simultaneously present in a detection volume and therefore registered as one single particle (Raasch and Umhauer, 1984). For enhanced aerosol concentration the true particle number concentration n_t can be determined from the measured particle number n_m (Jaenicke, 1970 and 1972; Hermann and Wiedensohler, 2001):

$$n_t = n_M \cdot \exp(n_t \cdot Q \cdot t) = n_M \cdot \exp(n_t \cdot c) \quad (1)$$

where: Q = volume flow rate in $cm^3\,s^{-1}$
t = residence time of a particle in the detector in s
c = coincidence parameter $Q \cdot t$ in cm^3.

This implicit function can be solved by a Taylor expansion of second order (Eq. 2) which causes an error of less than 2% for particle number concentrations up to

CC BY

5×10^4 cm^{-3} for the CPC TSI Model 7610 (Hermann and Wiedensohler, 2001).

$$n_t = \frac{1}{c^2}\cdot\left(\frac{1}{n_M}-c\right)-\sqrt{\left(\frac{1}{c^2}\cdot\left(\frac{1}{n_M}-c\right)\right)^2-\frac{2}{c^2}} \quad (2)$$

For higher particle number concentrations Eq. (1) can be solved iteratively (Jaenicke, 1970). Using Eq. (2), the coincidence parameter of the optical detector c=10^{-5} cm^{-3} (TSI Incorporated, 2002), and the volume flow rates and residence times of the COPAS CPCs (Table 4), the coincidence effect in the COPAS CPCs can be calculated. It can be concluded that at particle number densities below roughly 10^4 cm^{-3} coincidence is not seriously influencing the counting results. Such high concentrations are rarely encountered in the UT/LS. In cases the measured particle number concentration significantly exceeds 10^4 cm^{-3} the measurements with COPAS have to be corrected by a factor κ_C which is parameterized by κ_C=exp($1.23\times10^{-5}\times n_M$).

Auto-nucleation occurs in a CPC when the supersaturation of the working fluid vapour reaches the point that new particles are formed from the fluid's gas phase by homogeneous nucleation (e.g. Hämeri, et al. 1995). In particular, at low pressure conditions and for high temperature differences ΔT this effect can cause significant measurement errors. Furthermore, the occurrence of auto-nucleation depends on the specific CPC design. Therefore, the COPAS CPCs were studied concerning the probability that auto-nucleation generates new particles inside the instrument. Using the same calibration set-up as described in section 4 and by Hermann and Wiedensohler (2001), particle-free air was led to both COPAS instruments at an operating pressure of 50 hPa. The temperature difference ΔT was increased stepwise to check at which point auto-nucleation starts to occur. At 50 hPa significant particle concentrations, i.e. n>10 cm^{-3}, were not observed until a ΔT of 42°C was reached. At 100 hPa, auto-nucleation occurred only for ΔT>47°C. Therefore, for the range of temperature differences used for the COPAS instruments (17–33°C), the process of auto-nucleation can be excluded.

CC BY

6 The particle volatilization efficiency of the heated channel

The heating line is equipped with a temperature controller to keep the heating temperature stable within ±5% accuracy related to the setting of 250°C. The volatizing behavior of the COPAS heating line was studied by laboratory experiments using a pure H_2SO_4-H_2O calibration aerosol. To avoid contamination of the pure H_2SO_4-H_2O aerosol care was taken to work at very clean conditions. For instance, contaminations of gaseous ammonia are easily taken up by the acidic particles and reactions with H_2SO_4 form quickly ammonium sulfate ($(NH_4)_2SO_4$). Ammonium sulfate is not entirely evaporated at the temperature of 250°C inside the aerosol heating line and therefore artifacts may occur. Prior to the measurements, all inner surfaces of the stainless steel tubes of the calibration setup were treated with citric acid ($C_6H_8O_7$). High purity nitrogen (N_2) was used exclusively as the carrier gas for the particles. The H_2SO_4-H_2O particles were generated with a particle generator (Middlebrook et al., 1997; Böttger, 2000) by heating a small reservoir of 90 weight-percent solution of pure H_2SO_4 and H_2O.

The freshly generated polydisperse aerosol was separated with an electrostatic classifier (Model 3080N, TSI Incorporated) and the size-selected calibration aerosol was transferred into a variable low pressure sampling volume via a critical orifice. The COPAS-I instrument with one heated and one regular channel was connected to that aerosol chamber. For these experiments the results from the heated channel were compared with the measurements from the non-heated channel of the same COPAS instrument, where both channels have a d_{p50} of ~11 nm (see Fig. 5a and b). First studies at 70 hPa showed that particles with d_p=50 nm were volatilized to sizes smaller than the d_{p50} of COPAS-I already at heating temperatures of 176°C. To insure the total volatilization of particles with sizes d_p>50 nm the temperature of the COPAS aerosol heating line was set to 250°C. For three pressure conditions, i.e. 70 hPa, 150 hPa, and 300 hPa, the heating efficiency was characterized for pure H_2SO_4-H_2O aerosol particles in the size range of 20 nm<d_p<200 nm. The results of the heating line characterization are shown in Fig. 6. It can be concluded that at an operation temperature

AMTD
1, 321–374, 2008

of 250°C and over the pressure range 70–300 hPa the aerosol pre-heater volatilizes more than 98% of the H_2SO_4-H_2O particles. Although, we were not able to generate H_2SO_4-H_2O particles of sizes larger than 200 nm within this study it can be assumed from laboratory as well as field study experience that this volatilization efficiency of the aerosol pre-heater is also valid for particles with d_p>200 nm. This concept has been successfully applied for the differentiation of pure stratospheric sulphuric acid droplets from droplets containing residues of meteoric ablation (Curtius et al., 2005).

7 Characterization experiments during high altitude flight operation

A cross-correlation of the COPAS CPCs (see Fig. 7) was performed to demonstrate the coherence of the measurements and to provide in-flight quality control. Therefore the data of altogether six measurement flights were used when all three unheated COPAS channels were operated on the M-55 "Geophysica" with identical settings. During these flights all COPAS CPCs were operated with butanol as working fluid and with common differential temperature ΔT and therefore with the same cut-off diameters of $d_{p50}\approx$10 nm (Curtius et al., 2005). The correlations were obtained using 15-s running averaged data of particle number concentration by (1.) inter-comparing the two CPC channels contained inside COPAS-II (Fig. 7a) and by (2.) cross-comparing one CPC channel from COPAS-I with one channel from COPAS-II, respectively (Fig. 7b). In both cases the correlation coefficients with 0.996 (Fig. 7a) and 0.985 (Fig. 7b) illustrate a high level of consistency between the COPAS CPCs.

8 Examples of vertical profiles measured at arctic and tropical latitudes

In Fig. 8 vertical profiles of the particle number concentration of two randomly chosen flights demonstrate the outcome of measurements with the COPAS instruments and are used to discuss instrumental limitations dependent on the flight conditions, partic-

CC BY

ularly at low flight altitudes. In the graphs the particle number concentration is given as 15-s running averages, as an appropriate tool to increase the signal-to-noise ratio and to smooth the natural variability of recorded 1 Hz data. The potential temperature Θ is chosen as the vertical coordinate.

The upper panel of Fig. 8 depicts a flight on 2 February 2003 (longitude: 10°–30° east; latitude: 68°–76° north) at Arctic regions during the **EU**ropean **P**olar stratospheric cloud and **L**ee-wave **EX**periment (EUPLEX). During this campaign both COPAS instruments were commonly operated with the working fluid butanol. For a proof of concept COPAS-II was operated with differential temperatures ΔT yielding the same cut-offs of COPAS-I of d_{p50}=10 nm (cf. Sect. 7). In the lower panel of Fig. 8 data are shown from a flight on 12 February 2005 (longitude: 41°–51° west; latitude: 17°–21° south) during the **T**ropical **C**onvection, **CI**rrus and **N**itrogen **OX**ides Experiment (TROCCINOX), when both COPAS instruments were operated with FC-43 as the working fluid. The ΔT for each of the non-heated CPCs was set to yield different cut-off diameters of d_{p50}=6 nm (n_6), d_{p50}=11 nm (n_{11}), and d_{p50}=15 nm (n_{15}), respectively (cf. Sect. 4). COPAS-I measured the total number concentration n_{11} as well as the non-volatile particle number (n_{11} nv). On the right side of each panel the respective fraction of non-volatile particles is shown.

Comparing those results, the different measurement locations immediately become obvious. The tropical profiles, reaching the tropopause at Θ=380 K, clearly show a sharp step of particle number concentration, coincident for all unheated CPC channels, from 500–1000 cm^{-3} (<380 K) down to ~100 cm^{-3}. A further continuous decrease with increasing altitude down to 15–40 cm^{-3} at 445 K is observed. Altogether, the example from our tropical measurements shows very good agreement with previously published vertical particle distributions (e.g. Brock et al., 1995) up to UT/LS altitudes for undisturbed stratospheric conditions. The polar measurements show a relatively smooth transition of the particle concentration from 50–200 cm^{-3} in tropospheric air (Θ<370 K – influenced by air masses from lower latitudes) down to concentrations mainly below 40 cm^{-3} inside the polar winter vortex (Θ>380 K – nearly isolated from

CC BY

influences of lower latitudes). Above the tropopause, with increasing Θ, a continuous decrease of the particle number down to 10–20 cm^{-3} can be observed until 435 K – above this level the particle number increases again. From the profile of non-volatile aerosol fraction – with continuous increase with increasing Θ – the enhanced particle number at Θ>435 K is assumed to mainly contain refractory material (50–70%). Detailed discussions concerning the meteoric origin of this refractory aerosol material and the transport processes into the polar winter vortex are given by Curtius et al. (2005). Compared to the polar example the non-volatile particle fraction of the tropical measurements clearly decreases below 50% above the tropical tropopause, and above a transition region (Θ>400 K) a nearly constant value of about 25% for the refractory aerosol fraction is. While for the polar measurement the refractory material is discussed to be transported mainly from higher (mesospheric) altitudes with subsiding air masses into the polar winter vortex (Curtius et al., 2005), at tropical latitudes the non-volatile particle fraction has a vertically nearly constant value and is most likely maintained by transport processes between the Tropical Tropopause Layer (TTL) and the stratosphere (Hamill at al., 1997).

Figure 8 illustrates the operational limitations of COPAS. From the vertical profiles of both case studies it is obvious that the data do not extend down to ground level. The COPAS measurements from ground level to altitudes of 7–12 km have to be analyzed carefully regarding the data quality. For the particular cases measurement data from flight altitudes lower than 7.5 km (Θ=300 K for the polar measurement) and 11.5 km (Θ=350 K at tropical latitudes) were rejected if one of the following three aspects limited the COPAS measurements. For both COPAS instruments, independent on the measurement site, measurements are usually discarded between take-off and reaching flight altitudes of ∼7 km because the fast ascent rates of the M-55 "Geophysica" of 20–30 m s^{-1}, with the aim to reach UT/LS altitudes as fast as possible, generally cause the automated volume flow regulation of COPAS not to work properly. Turbulences occur in the flow system which severely limit the automatic flow metering and control if ascent or descent rates exceed 10 m s^{-1}.

AMTD
1, 321–374, 2008

The second aspect limiting the COPAS operation is given by high ambient temperatures at the ground prior to the flights. In particular at locations where ambient temperatures above 30°C occur on the airfield (cf. Fig. 2) the cooling system of COPAS condensers is not work efficiently immediately after take-off. As it is shown in Fig. 2 for the measurement example in tropical regions the oil temperature of the condenser cooling circuit remained clearly above a sufficient cooling temperatures of ∼10°C until the aircraft reached an altitude of 12 km. Consequently, data recorded below 12 km altitude had to be discarded because the correct temperature settings of the condenser were not reached.

A third limiting aspect of COPAS operation, with respect to low flight altitudes, is caused by the activation properties of the CPC working fluid FC-43 at ambient pressures >400 hPa (cf. Herrmann et al., 2005) – i.e. altitudes below ∼7 km. Above 400 hPa the CPC cut-offs as well as the maximum asymptotic counting efficiency can change significantly. Therefore, for increasing ambient pressure conditions (>400 hPa) enlarged uncertainties of the COPAS measurement data have to be considered.

Generally, for both cases, under arctic as well as tropical conditions, the aerosol preheating device worked properly during the complete missions. In particular, at artic conditions where during flight operation ambient temperatures never reached more than −20°C the pre-heating temperature was kept constant at 250°C with an uncertainty of less than ±5%.

9 Aerosol observation in M-55 "Geophysica" plumes

Several observations of enhanced particle number concentration during two research flights during the TROCCINOX and the SCOUT missions were caused by crossings of the M-55 "Geophysica's" own exhaust at altitudes between 16 and 18 km. The plumes were identified by simultaneous short term increases in the particle number concentrations and the concentrations of nitrogen oxides (NO_x=NO+NO_2) detected by the German Aerospace Center (DLR) using the chemiluminescence technique (Voigt et

CC BY

al., 2005). The NO_x instrument on board the M-55 "Geophysica" is described in detail by Voigt et al. (2006). We can exclude civil aviation as potential source of these particle and NO_x enhancements, as the plumes were detected at altitudes between 16 and 18 km, more than 4 km above the cruise altitudes of commercial aircraft. Additional confidence in the plume crossings was given by air mass back trajectories calculations similar to the method derived by Corti at al. (2008). This combined evidence from in situ data und trajectory modeling also suggests that it is unlikely, that the enhancements were caused by lightning.

The 1 Hz-time series of the particle number concentration measured with COPAS-II during a tropical flight on 5 February 2005 (longitude: 48°–54° west; latitude: 19°–22° south) of the TROCCINOX mission is shown in Fig. 9. The ultra-fine particle number concentration n_{6-15} (Fig. 9) is calculated and corrected for diffusional losses (κ_L =1.28, cf. Sect. 3.3 and Table 3). Two distinct increases, feature 1.1 and 1.2, in particle concentration occur in this time series. Due to instrumental background measurements of the NO_x instrument during feature 1.1 we refrain from a detailed discussion of feature 1.1. Feature 1.2 is caused by the crossing of a M-55 "Geophysica's" exhaust as is supported by simultaneous particle and NO_x enhancements. The plume age was estimated to be in the range of 8000 s as approximated by use of HYSPLIT data (**HY**brid **S**ingle-**P**article **L**agrangian **I**ntegrated **T**rajectory model – available at http://www.arl.noaa.gov/ready/hysplit4.html).

The second example is taken from a flight on 25 November 2005 (longitude: 127°–132° east; latitude: 9°–13° south) during the mission **S**tratosphere-**C**limate Links with Emphasis **O**n the **U**pper **T**roposphere and Lower Stratosphere (SCOUT-O_3). The 1 Hz-time series of corrected particle number concentrations is shown in Fig. 10 where three observations are denoted with feature 2.1, 2.2, and 2.3, respectively. In Fig. 11 the 2-D projection of the flight track is shown indicating high potential of exhaust crossing. The measurement flight was intended to investigate a single, overshooting convective cell. Only plume 2.3 can be supported by simultaneous observation of NO_x enhancements although the air mass trajectories for this event are suggestive of a lower probability of

CC BY

contrail match than feature 2.1 and 2.2. Therefore, we focus on feature 2.3 in further analyses with an estimated plume age in the order of 2600 s.

We determined the particle emission indices $EI[n]$ of the M-55 aircraft engines at UT/LS conditions using the measured enhancements in NO_x mixing ratios inside aircraft exhaust as a normalizing factor. This method has already been applied for other aircraft (Fahey et al., 1995a, b, Schlager et al., 1997; Anderson, et al., 1999), particularly for plume ages in the range of hours. The $EI[n]$ of an aircraft engine, in units of particle number per kg fuel burned, was calculated by using Eq. (3) (Anderson et al., 1999).

$$EI[n_i] = \left(\frac{\Delta n_i}{\Delta NO_x}\right) \cdot EI[NO_x] \cdot \frac{M_{air}}{\left(\rho \cdot M_{NO_2}\right)} \quad (3)$$

where: Δn_i = particle number concentration in the plume related to background concentrations in cm^{-3}, the index i distinguishes the CPC cut-off sizes.
Δ NO_x = differential NO_x mixing ratio in the plume related to background values, in ppt.
M = molecular Mass, M_{air}=29 u, M_{NO_2}=46 u.
ρ = air density, in kg m^{-3}, at flight conditions during observed event.

The integrated signal (ΔX) of observed enhancement of a species **X** related to background conditions is given as:

$$\Delta X = \Delta t_{obs} \left(X_{plume} - X_0\right) \quad (4)$$

Here, Δt_{obs} is the duration of an enhancement observation and the bracket term is the difference of measured number concentrations, or mixing ratio, inside the plume (X_{plume}) related to background conditions outside the plume (X_0).

The $EI[NO_x]$ for the M-55 "Geophysica" has to be estimated from a comparison with the $EI[NO_x]$ of the NASA ER-2 aircraft, determined from ground-based experiments by Fahey et al. (1995b). The M-55 "Geophysica" is a double-engine aircraft (2 × Aviadvigatel D-30-V12) compared to the NASA ER-2 with a single turbine engine (Pratt

CC BY

and Whitney J75). According to the specifications of the engine manufacturer the fuel consumption of the NASA ER-2 at flight condition is determined to be 727 kg h^{-1} with resulting $E/[NO_x]_{ER\text{-}2}$=3.6–4.3 g kg^{-1} (Fahey et al., 1995b). The fuel consumption of the M-55 "Geophysica" is recorded during the flights (in 1 Hz time resolution) and averaged for the consumption when the emission occurred for each plume event. For the emission time period related to feature 1.2 the mean fuel consumption for both engines together equals 1518 kg h^{-1} during ascent near 16 km altitude, which indicates an enhanced $E/[NO_x]_{M\text{-}55}$ due to engine's full-load operation. At cruising flight conditions the $E/[NO_x]$ of both aircraft might be equal. Nevertheless, the full-load operation of aircraft engines might increase the fuel-to-oxygen ratio inside the turbines, causing inefficient fuel burning, which affects increased emission indices compared to cruising conditions. For feature 2.3 the determined fuel consumption equals 846 kg h^{-1} in total for both engines at cruising altitude (19 km). As an approximation for this study only, the NO_x emission index for the M-55 "Geophysica" is estimated to range between $E/[NO_x]_{M\text{-}55}$=1–1.5·$E/[NO_x]_{ER\text{-}2}$=3.6–6.5 g kg^{-1} which is comparable with published NO_x emission indices for small aircraft, e.g. the DLR Attas VFW-614 with $E/[NO_x]_{Attas}$≈7 g kg^{-1}, or the Boeing B737 with $E/[NO_x]_{B737}$=9.4–11.4 g kg^{-1} (Schulte et al., 1997), the Boeing B727 with $E/[NO_x]_{B727}$=7.7 g kg^{-1} (Schumann et al., 1998).

n_6, n_{15}, and the ultra-fine particle number concentration n_{6-15} were used to determine the $E/[n_i]_{M\text{-}55}$ from the plume 1.2 encounter and related background concentrations n_o, outside of the plume: n_6 = 1930 cm^{-3}(for n_o=220 cm^{-3}), n_{15}=880 cm^{-3} (for n_0=180 cm^{-3}), and n_{6-15}=1050 cm^{-3} (for n_o=50 cm^{-3}), as the respective maxima of particle enhancement occurring for a duration of 5 s. In total the observed particle enhancement, but with lower magnitude related to the background, last about 18 s. The NO_x enhancement with ΔNO_x=150 ppt was observed simultaneously over 20 s within the plume (at current flight speed correspondent to a distance of 3.3 km).

Measured maxima of the n_i during the plume 2.3 observation during 3 seconds are n_6=1910 cm^{-3} and n_{15}=1280 cm^{-3} (both for n_o=47 cm^{-3}), n_{6-15}=830 cm^{-3}

AMTD
1, 321–374, 2008

at a background concentration of <10 cm^{-3}, n_{11}=1820 cm^{-3} (for n_o=50 cm^{-3}) and n_{11} nv=990 cm^{-3} (for n_o=25 cm^{-3}). Here the observed NO_x enhancement delivers ΔNO_x = 80 ppt for 25 seconds (flight distance of about 4.7 km).

The determined $EI[n_i]_{M\text{-}55}$ in the range of 1.4–8.4×10^{16} particles per kg fuel are listed in Table 5 for both cases, together with results for the NASA ER-2 for similar plume ages (Anderson et al., 1999), and the supersonic civil aircraft Concorde (Fahey et al., 1995a) – using two examples of aircraft reaching similar flight altitudes as the M-55 "Geophysica". Generally, it can be seen that the $EI[n_i]$ for both the M-55 "Geophysica" and the NASA ER-2 show results of the same magnitude. However, an uncertainty of ±50% has to be considered for the calculated $EI\,[n_i]_{M\text{-}55}$ mainly caused by the uncertainty of estimated $EI[NO_x]_{M\text{-}55}$ (assumed to be the largest uncertainty compared to the accuracy of the particle measurement or the nitrogen oxide detection). Additional uncertainty is given if for one of the plume events, or both, the M-55 "Geophysica" flight path did not exactly cross the plume's core. Furthermore, of course, the processing of aerosol particles, particularly in the ultra-fine size mode, within a time span of up to 8000 s has significant influence on the accuracy of calculated $EI[n_i]_{M\text{-}55}$. Despite large uncertainties, our analysis presents a first estimate of the $EI[n_i]_{M\text{-}55}$ for the high altitude research aircraft Geophysica.

10 Conclusions

The operation principle and a characterization of the two **CO**ndensation **PA**rticle counting **S**ystems (COPAS) for aircraft-based measurements on board the high altitude research aircraft M-55 "Geophysica" was presented in this work. The two COPAS instruments, designed for aerosol concentration measurements in the UT/LS region, include two CPCs each. The operation of three of those CPC channels allows for measurements of the particle number concentration with different threshold diameters. Thereby the number concentration of ultra-fine, freshly nucleated particles can be derived. The

CC BY

fourth CPC channel is operated with an aerosol pre-heater to quantify the refractory fraction of the aerosol particles.

The performance of the COPAS aerosol inlet, constructed for application on board the Russian high altitude research aircraft M-55 "Geophysica", has been discussed with respect to aspiration, transmission, and transport. Concerning aspiration and transmission of the COPAS aerosol inlet it is estimated that particles with diameter of up to a few micrometers enter the aerosol inlet and pass the aerosol lines without significant particle losses. However, concerning the transmission efficiency of the aerosol inlet, only additional wind tunnel studies can provide a complete characterization. Furthermore, within such wind tunnel studies, it should be investigated how the inlet aspiration and transmission efficiency can be optimized by use of a shroud as it is used for many other airborne aerosol measurements (Baumgardner et al., 1991; Murphy and Schein, 1998; Twohey, 1998; Weber et al., 1998). Finally, particle losses inside the inlet system are assumed to be negligible for particle sizes smaller than 500 nm, particularly considering more significant uncertainties given by the counting efficiency of the CPCs.

The counting efficiency as a function of particle size and pressure was determined for each of the four COPAS CPC channels. The result of this CPC characterization allows to set the cut-offs to different particle sizes. For our measurements, the cut-off sizes were typically set to d_{p50}=6 nm (COPAS-II-2), d_{p50}=11 nm (COPAS-I-2) and d_{p50}=15 nm (COPAS-II-1). From the different readings of the three counters, recent nucleation events can be identified by differentiation. The aerosol pre-heater (upstream of COPAS-I-1 with d_{p50}=11 nm), which was characterized with respect to its ability to completely vaporize pure H_2SO_4-H_2O droplets, allows for physico-chemical aerosol studies concerning the volatility of the UT/LS aerosol. A pre-heating temperature of 250°C was chosen to volatilize the main component of UT/LS aerosol, namely H_2SO_4-H_2O. These volatility investigations are related to the stratospheric refractory aerosol components which might have a substantial influence on the stratospheric aerosol properties and heterogeneous chemistry in the stratosphere.

With several case studies the performance of the COPAS instruments, even under

CC BY

extreme ambient conditions, was demonstrated. Cross- correlations of two COPAS channels, for two channels of the same COPAS and for two channels of two independent COPAS instruments, illustrate the high consistency of the COPAS measurements. Two randomly chosen flight examples were used to describe possible outcome of the COPAS measurements and, furthermore, the instrumental limitations with respect to flight altitude.

Enhanced ascent and descent rates of the measurement platform are an important issue having significant impact on the performance of the COPAS particularly at lowermost flight altitudes. Ascent and descent rates exceeding 10 m s^{-1} up to flight altitudes of 7–12 km significantly impact the reliability of COPAS measurements. Other ambient conditions, with far-reaching impact on the measurement performance of COPAS, are given by ambient air temperatures. Generally, cooling circuit oil temperatures of >10°C force the differential temperature of the COPAS CPCs to deviate from the settings which the instrument is calibrated for. Measurements made on deviated CPC temperatures are corrupt and they have to be rejected from analysis. Ground air temperatures of up to 15°C have minimal influence.

Finally, particle emission indices $EI[n_i]_{\text{M-55}}$ were estimated for the M-55 "Geophysica" from two plume crossings as indicated by enhanced particle number concentrations and simultaneously increased NO_x mixing ratios. The derived $EI[n_i]_{\text{M-55}}$ are comparable to results of the NASA ER-2, nevertheless accuracy of estimated $EI[n_i]_{\text{M-55}}$ ranges within ±50%. Further, it could be shown that due to the independent CPC channels with different cut-offs the COPAS instruments are generally able to deliver size-segregating measurements with high time resolution to carry out such studies of short events.

Acknowledgements. We are thankful to V. Dreiling and C. Schrörs for their earlier preparatory work with the original COPAS, F. Helleis, M. Flanz, and W. Schneider for the development of the COPAS electronics and to K.-H. Bückart and the mechanical workshop of the MPI-Chemistry for technical support. We thank Stefano Balestri, APE-GAIA, the entire M-55 "Geophysica" crew, and the pilots in particular. Also the significant and crucial technological support of J. C. Wilson (University of Denver, Colorado, USA) and C. A. Brock (NOAA Laboratories,

Boulder, Colorado, USA) for design and aircraft implementation are gratefully acknowledged. This work was supported by the European research projects EUPLEX (EVK2-2001-00084), APE-Infra (EVR1-CT-2001-40020), TROCCINOX (EVK2-2001-00122), and SCOUT-O_3 (GOCE-CT-2004-505390). The work of C. Voigt was funded by the HGF in the frame of the Junior Research Group AEROTROP. We thank T. Corti for trajectory calculations and H. Schlager for providing NO_x data.

This Open Access Publication is financed by the Max Planck Society.

References

Anderson, B. E., Corer, W. R., Crawford, J., Gregory, G. L., Vay, S. A., Brunke, K. E., Kondo, Y., Koike, M., Schlager, H., Baughcum, S. L., Jensen, E., Yongjing Zhao, and Kazuyuki Kita: An assessment of aircraft as a source of particles to the upper troposphere, J. Geophys. Res., 26, 20, 3069–3072, 1999.

Ansmann, A., Wagner, F., Wandinger, U., Mattis, I., Görsdorf, U., Dier, H.-D., and Reichardt, J.: Pinatubo aerosol and stratospheric ozone reduction: Observations over central Europe, J. Geophys. Res., 1001, 18 775–18 785, 1996.

Arnold, F., Curtius, J., Speng, S., Deshler, T.: Stratospheric aerosol sulfuric acid: First in situ measurements using a novel balloon-based mass spectrometer apparatus, J. Atmos. Chem., 30, 3–10, 1998.

Baron, P. A. and Willeke, K.: Aerosol Measurement: Principles, Techniques, and Applications, 2nd Ed., John Wiley & Sons, New York, 2001.

Baumgardner, D., Huebert, B., and Wilson, C.: Meeting review: Airborne aerosol inlet workshop, NCAR Technical Note TN-362 + 1A, 288 pp., 1991.

Bengtsson, L.: Geo-Engineering to confine climate change: Is it all feasible?, An editorial comment, Climatic Change, 77, 229–234, doi:10.1007/s10584-006-9133-3, 2006.

Borrmann, S., Solomon, S., Dye, J. E., Baumgardner, D., Kelly, K. K., and Chan, K. R.: Heterogeneous reactions on stratospheric background aerosol, volcanic sulfuric acid droplets, and type 1 polar stratospheric clouds: Effect of temperature fluctuations and differences in particle phase, J. Geophys. Res., 102(D3), 3639–3648, 1997.

Borrmann, S., Thomas, A., Rudakov, V., Yushkov, V., Lepuchov, B., Deshler, T., Vinnichenko, N., Khattatov, V., and Stefanutti, V: Stratospheric aerosol measurements in the arctic winter of 1996/1997with the M-55 Geophysica high-altitude research aircraft, Tellus, 52B, 1088–1103, 2000.

Böttger, T: Aufbau einer Anlage zur Beschichtung luftgetragener Aerosolpartikel mit H_2O und H_2SO_4, Diploma thesis at the Faculty of Mechanical Engineering, University of Applied Sciences, Aachen, 2000.

Brock, C. A., Hamill, P., Wilson, J. C., Jonsson, H. H., and Chan, K. R.: Particle formation in the upper Tropical Troposphere: A source of nuclei for the stratospheric aerosol, Science, 270, 1650–1653, 1995.

Cicerone, R. J.: Geoengineering: Encouraging research and overseeing implementation; An editorial comment, Climatic Change, 77, 221–226, doi:10.1007/s10584-006-9102-x, 2006.

Cofer, W. R., Anderson, B. E., Winstead, E. L., and Bagwell, D. R.: Calibration and demonstration of a condensation nuclei counting system for airborne measurements of aircraft exhausted particles, Atmos. Environ., 32, 169–177, 1998.

Corti, T., Luo, B. P., de Reus, M., Brunner, D., Cairo, F., Mahoney, M. J., Martucci, G., Matthey, R., Mitev, V., dos Santos, F. H., Schiller, C., Shur, G., Sitnikov, N. M., Spelten, N., Vössing, H. J., Borrmann, S., and Peter, T.: Unprecedented evidence for deep convection hydrating the tropical stratosphere, Geophys. Res. Lett., 35, L10810, doi:10.1029/2008GL033641, 2008.

Curtius, J., Sierau, B., Arnold, F., Baumann, R., Busen, R., Schulte, P., and Schumann, U.: First direct sulfuric acid detection in the exhaust of a jet aircraft in flight, Geophys. Res. Lett., 25, 6, 923–926, 1998.

Curtius, J., Weigel, R., Vssing, H.-J., Wernli, H., Werner, A., Volk, C.-M., Konopka, P., Krebsbach, M., Schiller, C., Roiger, A., Schlager, H., Dreiling, V., and Borrmann, S.: Observations of meteoric material and implications for aerosol nucleation in the winter Arctic lower stratosphere derived from in situ particle measurements, Atmos. Chem. Phys., 5, 3053–3069, 2005,
http://www.atmos-chem-phys.net/5/3053/2005/.

Crutzen, P. J.: Albedo enhancement by stratospheric sulfur injections: a contribution to resolve

a policy dilemma?; An editorial essay, Climatic Change 77, 211–219, doi:10.1007/s10584-006-9101-y, 2006.
Cziczo, D. J., Thomson, D. S., and Murphy, D. M.: Ablation, flux, and atmospheric implications of meteors inferred from stratospheric aerosol, Science, 291, 1772–1775, 2001.
Deshler, T., Johnson, B. J., and Rozier, W. R.: Balloonborne measurements of Pinatubo aerosol during 1991 and 1992 at 41° N: Vertical profiles, size distribution, and volatility, Geophys. Res. Lett., 20, 1435–1438, 1993.
Deshler, T., Hervig, M. E., Kröger, C., Hofmann, D. J., Rosen, J. M., and Liley, J. B.: Thirty years of in situ stratospheric aerosol size distribution measurements from Laramie, Wyoming (41°N), using balloonborne instruments, J. Geophys. Res., 108, 4167, doi:10.1029/2002JD002514, 2003.
Dreiling, V. and Jaenicke, R.: Aircraft measurement with condensation nuclei counter and optical counter, J. Aerosol Sci., 19, 1045–1050, 1988.
Fahey, D. W., Keim, E. R., Boering, K. A., Brock, C. A., Wilson, J. C., Jonsson, H. H., Anthony, S., Hanisco, T. F., Wennberg, P. O., Miake-Lye, R. C., Salawitch, R. J., Louisnard, N., Woodbridge, E. L., Gao, R. S., Donnelly, S. G., Wamsley, R. C., Del Negro, L. A., Solomon, S., Daube, B. C., Wofsy, S. C., Webster, C. R., May, R. D., Kelly, K. K., Loewenstein, M., Podolske, J. R., and Chan, K. R.: Emission Measurements of the Concorde Supersonic Aircraft in the Lower Stratosphere, Science, 270, 5233, doi:10.1126/science.270.5233.70, 1995a.
Fahey, D. W., Keim, E. R., Woodbridge, E. L., Gao, R. S., Boering, K. A., Daube, B. C., Wofsy, S. C., Lohmann, R. P., Hintsa, E. J., Dessler, A. E., Webster, C. R., May, R. D., Brock, C. A., Wilson, J. C., Miake-Lye, R. C., Brown, R. C., Rodriguez, J. M., Loewenstein, M., Proffitt, M. H., Stimpfle, R. M., Bowen, S. W., and Chan, K. R.: In situ observations in aircraft exhaust plumes in the lower stratosphere at midlatitudes, J. Geophys. Res., 100(D2), 3065–3074, 1995.
Hamill, P., Jensen, E. J., Russel, P. B., and Bauman, J. J.: The life cycle of stratospheric aerosol particles, B. Am. Meteorol. Soc., 78, 1395–1410, 1997.
Hangal, S. and Willeke, K.: Overall efficiency of turbular inlets sampling at 0-90 degrees from horizontal aerosol flows, Atmos. Environ., 24A, 2379–2386, 1990.
Hämeri, K., Augustin, J., Kulmala, M., Vesala, T., Mäkelä, J., Aalto, P., and Krissinel, E.: Evaluation of homogeneous droplet formation inside UCPC (TSI Model 3025), J. Aerosol Sci., 26, 1003–1008, 1995.

Heintzenberg, J. and Ogren, J. A.: On the operation of the TSI-3020 condensation nuclei counter at altitudes up to 10 km, Atmos. Environ., 19, 1385–1387, 1985.
Hermann, M., Stratmann, F., Wilck, M., and Wiedensohler, A.: Sampling Characteristics of an Aircraft-Borne Aerosol Inlet System, J. Atmos. Ocean. Tech., 18, 7–19, 2001.
Hermann, M. and Wiedensohler, A.: Counting efficiency of condensation particle counters at low-pressure with illustrative data from the upper troposphere, J. Aerosol Sci., 32, 975–991, 2001.
Hermann, M., Adler, S., Caldow, R., Stratmann, F., and Wiedensohler, A.: Pressure-dependent efficiency of a condensation particle counter operated with FC-43 as working fluid, J. Aerosol Sci., 36, 11, 1322–1337, 2005.
Hinds, W. C.: Aerosol technology - properties, behaviour, and measurement of airborne particles, 2nd Ed., John Wiley & Sons, Inc., New York, 1999.
Hofmann, D. J. and Solomon, S.: Ozone destruction through heterogeneous chemistry following the eruption of El Chichón, J. Geophys. Res., 94, 5029–5041, 1989.
Holton, J. R., Haynes, P. H., McIntyre, M. E., Douglass, A. R., Rood, R. B., and Pfister, L.: Stratospheric-tropospheric exchange, Rev. Geophys., 33, 403–439, 1995.
Jaenicke, R.: Untersuchung von Geräten zur Messung der Größenverteilung großer Aerosolteilchen in anthropogen nicht beeinflußten Atmosphären, Dissertation at the Faculty of Natural Science, Johannes Gutenberg-University, Mainz, 1970.
Jaenicke, R.: The optical particle counter. Cross-sensitivity and coincidence, J. Aerosol Sci., 30., 95–111, 1972.
Jaenicke, R. and Kanter, H. J.: Direct condensation nuclei counter with automatic photographic recording, and general problems of "absolute" counters, J. Appl. Meteorol., 15, 620–632, 1976.
Jònsson, H. H., Wilson, J. C., and Brock, C. A.: Evolution of the stratospheric aerosol in the northern hemisphere following the June 1991 volcanic eruption of Mount Pinatubo: Role of the tropospheric-stratospheric exchange transport, J. Geophys. Res., 101, 1553–1570, 1996.
Junge, C.: Neuere Untersuchungen an großen atmosphärischen Kondensationskernen, Meteorol. Z., 52, 467–470, 1935.
Junge, C. E., Chagnon, C. W., and Manson, J. E.: A world-wide stratospheric aerosol layer, Science, 133, 1478–1479, 1961.
Junge, C. E.: Vertical profiles of condensation nuclei in the stratosphere, J. Meteorol., 18,

505–509, 1961.
Junge, C. E. and Manson, J. E.: Stratospheric Aerosol Studies, J. Geophys. Res., 66, 7, 2163–2182, 1961.
Kulmala, M., Riipinen, I., Sipilä, M., Manninen, H. E., Petäjä, T., Junninen, H., Dal Maso, M., Mordas, G., Mirme, A., Vana, M., Hirsikko, A., Laakso, L., Harrison, R. M., Hanson, I., Leung, C., Lehtinen, K. E. J., and Kerminen, V.-M.: Toward direct measurement of atmospheric nucleation, Science, 318, 5847, 89–92, doi:10.1126/science.1144124, 2007.
Kürten, A., Curtius, J., Nillius, B., and Borrmann, S.: Characterization of an automated, water-based expansion condensation nucleus counter for ultra-fine particles, Aerosol Sci. Tech., doi:10.1080/02786820500431355, 2005.
McMurry, P. H.: The history of condensation nucleus counters, Aerosol Sci. Tech., 33, 297–322, 2000.
Middlebrook, A. M., Thomson, D. S., and Murphy, D. M.: On the purity of laboratory-generated sulfuric acid droplets and ambient particles studied by laser mass spectrometry, Aerosol Sci. Tech., 27, 293–307, 1997.
Minikin, A., Petzold, A., Ström, J., Krejci, R., Seifert, M., Velthoven, P. v., Schlager, H., and Schumann, U.: Aircraft observation of upper tropospheric fine particle aerosol in the northern an southern hemisphere at midlatitudes, Geophys. Res. Lett., 30, 1503–1509, 2003.
Murphy, D. M. and Schein, M. E.: Wind tunnel tests of a shrouded aircraft inlet, Aerosol Sci. Tech., 28, 33–39, 1998.
Murphy, D. M., Thompson, D. S., and Mahoney, M. J.: In situ measurements of organics, meteoritic material, mercury, and other elements in aerosols at 5 to 19 kilometers, Science, 282, 1664–1669, 1998.
Murphy, D. M., Hudson, P. K., Thompson, D. S., Sheridan, P. J., and Wilson, J. C.: Observations of Mercury-Containing Aerosols, Environ. Sci. Technol., 40, 3163–3167, 2006.
Murphy, D. M., Cziczo, D. J., Hudson, P. K., and Thompson, D. S.: Carbonaceous material in aerosol particles in the lower stratosphere and tropopause region, J. Geophys. Res., 112, D04203, doi:10.1029/2006JD007297, 2007.
Myasishchev Design Bureau: High-altitude M55 Geophysica aircraft, Handbook, 3rd Ed., Myasishchev Design Bureau, Moskau, 2002.
Noone, K. J. and Hansson, H.-C.: Calibration of the TSI 3760 condensation nucleus counter for non-standard operating conditions, Aerosol Sci. Tech., 13, 478–485, 1990.
Notholt, J., Kuang, Z., Rinsland, C. P., Toon, G. C., Rex, M., Jones, N., Albrecht, T., Deckel-

mann, H., Krieg, J., Weinzierl, C., Bingemer, H., Weller, R., and Schrems, O.: Enhanced upper tropical tropospheric COS: Impact on the stratospheric aerosol layer, Science, 300, 307–310, 2003.
Peter, T.: Microphysics and heterogeneous chemistry of polar stratospheric clouds, Annu. Rev. Phys. Chem., 48, 785–822, 1997.
Raasch, J. and Umhauer, H.: Errors in the determination of particle size distributions caused by coincidence in optical particle counter, Part. Part. Syst. Char., 1, 53–58, 1984.
Rosen, J. M.: The boiling point of stratospheric aerosols, J. Appl. Meteorol., 10, 1044–1045, 1971.
Saros, M. T., Weber, R. J., Marti, J. J., and McMurry, P. H.: Ultra-fine aerosol measurement using a condensation nucleus counter with pulse height analysis, Aerosol Sci. Tech., 25, 200–213, 1996.
Schlager, H., Konopka, P., Schulte, P., Schumann, U., Ziereis, H., Arnold, F., Klemm, M., Hagen, D. E., Whitefield, P. D., and Ovarlez, J.: In situ observations of air traffic emission signatures in the North Atlantic flight corridor, J. Geophys. Res., 102(D9), 10 739–10 750, 1997.
Scholz, V. J.: Ein neuer Apparat zur Bestimmung der Zahl der geladenen und ungeladenen Kerne, Z. Instrumentenkd., 51, 505–522, 1931.
Scholz, V. J.: Vereinfachter Bau eines Kernzählers; Meteorol. Z., 49, 381–388, 1932.
Schumann, U., Schlager, H., Arnold, F., Baumann, R., Haschberger, P., and Klemm, O.: Dilution of aircraft exhaust plumes at cruise altitudes, Atmos. Environ., 32(18), 3097–3103, 1998.
Sgro, L. A. and de la Mora, J. F.: A simple turbulent mixing CNC for charged particle detection down to 1,2 nm, Aerosol Sci. Tech., 38, 1–11, 2004.
Sipilä, M., Lehtipalo, K., Kulmala, M., Petäjä, T., Junninen, H., Aalto, P. P., Manninen, H. E., Kyr, E.-M., Asmi, E., Riipinen, I., Curtius, J., Krten, A., Borrmann, S., and O'Dowd, C. D.: Applicability of condensation particle counters to measure atmospheric clusters, Atmos. Chem. Phys., 8, 4049–4060, 2008, http://www.atmos-chem-phys.net/8/4049/2008/.
SPARC, Assessment of Stratospheric Aerosol Properties (ASAP), Thomason, L., and Peter, T. (Eds.): SPARC Report No.4, WMO/ICSU/IOC World Climate Research Programme, http://www.atmosp.physics.utoronto.ca/SPARC/PublicationIndex.html, 2006.
Spurny, K. R.: Atmospheric condensation nuclei. P. J. Coulier 1875 and J. Aitken 1880, (Historical Review), Aerosol Sci. Tech., 32, 243–248, 2000.
Szymanski, W. and Wagner, P. E.: Aerosol size distribution during a condensational growth pro-

cess. Measurements and comparison with theory, Atmos. Environ., 17, 2271–2276, 1983.
Thomas, A., Borrmann, S., Kiemle, C., Cairo, F., Volk, M., Beuermann, J., Lepuchov, B., Santacesaria, V., Matthey, R., Radukov, V., Yushkov, V., MacKenzie, A. R., and Stefanutti, L.: In situ measurements of background aerosol and subvisible cirrus in the tropical tropopause region, J. Geophys. Res., 107, 4763, doi:10.1029/2001JD001385, 2002.
TSI Incorporated: Model 3760A/3762 Condensation Particle Counter – Instruction Manual, Revision D, TSI Incorporated, 2002.
TSI Incorporated: Model 3068A Aerosol Electrometer – Instruction Manual, Revision K, TSI Incorporated, 2003.
Turco, R. P., Whitten, R. C., and Toon, O. B.: Stratospheric Aerosols: Observation and theory, Rev. Geophys. Space GE, 20, 233–279, 1982.
Twohey, C. H.: Model calculations and wind-tunnel testing of an isokinetic shroud for high-speed sampling, Aerosol Sci. Tech., 29, 261–280, 1998.
Voigt, C., Schreiner, J., Kohlmann, A., Zink, P., Mauersberger, K., Larsen, N., Deshler, T., Kröger, C., Rosen, J., Adriani, A., Cairo, F., Di Donfrancesco, G., Viterbini, M., Ovarlez, J., Ovarlez, H., David, C., and Dörnbrack, A.: Nitric Acid Trihydrate (NAT) in Polar Stratospheric Clouds, Science, 290, 1756–1758, 2000.
Voigt, C., Schlager, H., Luo, B. P., Dörnbrack, A., Roiger, A., Stock, P., Curtius, J., Vössing, H., Borrmann, S., Davies, S., Konopka, P., Schiller, C., Shur, G., and Peter, T.: Nitric Acid Trihydrate (NAT) formation at low NAT supersaturation in Polar Stratospheric Clouds (PSCs), Atmos. Chem. Phys., 5, 1371–1380, 2005, http://www.atmos-chem-phys.net/5/1371/2005/.
Voigt, C., Schlager, H., Ziereis, H., Kärcher, B., Luo, B. P., Schiller, C., Krämer,M., Popp, P. J., Irie, H., and Kondo, Y.: Nitric acid in cirrus clouds, Geophys. Res. Lett., 33, L05803, doi:10.1029/2005GL025159, 2006.
Wagner, P. E.: Aerosol growth by condensation, in: Aerosol Microphysics II, edited by: W. H. Marlow, Springer, Berlin, 1982.
Walter, S.: Simulation der Umströmung eines Teilstromentnahme-Einlasssystems für Höhenforschungsflugzeuge, Diploma thesis at the Institute for Physics of the Atmosphere, Johannes Gutenberg-University, Mainz, 2004.
Weber, R. J., Clark, A. D., Litchy, M., Li, J., Kok, G., Schillawski, R. D., and McMurry, P. H.: Spurious aerosol measurements when sampling from aircraft in the vincinity of clouds, J. Geophys. Res., 103, 28 337-28 346, 1998.

Weigel, R.: Ultrafeine Aerosolpartikel in der Stratosphäre: Charakterisierung eines Kondensationskernzählers und in-situ-Messungen in polaren, mittleren und tropischen Breiten, Dissertation at the Faculty of Physics, Johannes Gutenberg – University, Mainz, Germany, 2005.

Wilson, J. C., Hyun, J. H., and Blackshear, E. D.: The function and response of an improved stratospheric condensation nucleus counter, J. Geophys. Res., 88, 6781–6785, 1983.

Wilson, J. C., Stolzenburg, M. R., Clark, W. E., Loewenstein, M., Ferry, G. V., Chan, K. R., and Kelly, K. K.: Stratospheric sulfate aerosol in and near the northern hemisphere polar vortex: The morphology of the sulfate layer, multimodal size distribution, and the effect of denitrification, J. Geophys. Res., 97, 7997–8013, 1992.

Wilson, J. C., Jonsson, H. H., Brock, C. A., Toohey, D. W., Avallone, L. M., Baumgardner, D., Dye, J. E., Poole, L. R., Woods, D. C., DeCoursey, R. J., Osborn, M., Pitts, M. C., Kelly, K. K., Chan, K. R., Ferry, G. V., Loewenstein, M., Podolske, J. R., and Weaver, A.: In situ observations of aerosol and chlorine monoxide after the 1991 eruption of mount Pinatubo: effect of reactions on sulfate aerosol, Science, 216, 1140–1143, 1993.

WMO, World Meteorological Organization: Scientific assessment of ozone depletion: 1994, Report Nummer 37, 1995.

Yang, J.: Condensational growth of atmospheric aerosol particles in an expanding water saturated air flow: Numerical optimisation and experiment, Dissertation at the Faculty of Physics, Johannes Gutenberg-University, Mainz, 1999.

Zhang, Z. Q. and Liu, B. Y. H.: Dependence of the performance of TSI 3020 condensation nucleus counter on pressure, flow rate and temperature, Aerosol Sci. Tech., 13, 493–504, 1990.

Zhang, Z. Q. and Liu, B. Y. H.: Performance of TSI 3760 Condensation Nuclei Counter at reduced pressure and flow rates, Aerosol Sci. Tech., 15, 228–238, 1991.

Table 1. Particle losses (in %) as a function of particle size inside aerosol tubes as a function of atmospheric pressure for the three regular (non-heated) COPAS channels and for the COPAS channels with pre-heated aerosol line with variable inner diameter (from 6 mm to 12 mm and back to 6 mm) – determined from calculations according to Baron and Willeke (2001).

pressure in hPa	particle diameter in nm											
	6	8	10	12	14	16	18	20	35	50	100	1000
regular channels												
70	65	50	41	34	29	25	22	20	10	7	3	<1
300	51	39	31	25	21	19	16	14	7	5	2	<1
600	47	36	28	23	20	17	15	13	6	4	2	<1
pre-heated channel												
70	95	85	74	65	57	50	45	41	23	16	7	1
300	85	71	60	51	44	39	35	31	17	12	6	1
600	82	67	56	48	41	36	32	29	16	11	5	1

AMTD
1, 321–374, 2008

Table 2. Pressure dependent particle losses (in %) inside the aerosol tubes. Resulting correction factor κ_L are exclusively used for the ultra-fine size fraction n_{6-15} determined from results of COPAS-II.

pressure in hPa	particle diameter in nm									resulting κ_L
	6	7	8	9	10	11	12	14	15	
70	36	30	26	23	20	18	16	14	13	1.28
150	31	26	22	20	17	16	14	12	11	1.23
300	26	22	19	17	15	13	12	10	9	1.19
400	22	19	16	14	13	11	10	8	7	1.15

CC BY

Table 3. Resulting lower threshold diameters of each COPAS channel obtained from the experimental CPC characterization studies at two operating pressure conditions and with Ag-particles.

pressure in hPa	d_{p50} (in nm)$\pm\bar{\sigma}_{\eta}$ (in nm)			
	COPAS-I channel		COPAS-II channel	
	1	2	1	2
70	12.4±1.8	9.5±1.1	12.3±0.6	6.0±0.3
300	11.1±1.0	10.6±0.7	18.8±0.9	6.6±0.2

CC BY

Table 4. Pressure dependent volume flow rates for the COPAS CPCs and according residence times for the aerosol particles inside the photo-optical detector volume.

pressure p in hPa	volume flow Q in $cm^3\ s^{-1}$	residence time t in μs
70	16.4	0.6
150	10.1	1
300	6.1	1.5
600	4	2.5

Table 5. Particle EI values for the M-55 "Geophysica" estimated from two crossings of the own exhaust plume at different plume ages (pa) in relation to according EI of other high altitude reaching aircraft, the NASA ER-2 (Anderson et al., 1999) and the Concorde (Fahey et al., 1995a) – other CPC cut-offs than given for COPAS are denoted within brackets behind the EI value.

$EI[n_i]\times10^{16}$ kg^{-1} fuel burned	M-55 "Geophysica" feature 1.2 pa: 8000 s	M-55 "Geophysica" feature 2.3 pa: 2600 s	NASA ER-2 pa:~8000 s	NASA ER-2 pa:~2600 s	Concorde averages for pa: 960–3480
$EI[n_6]$	3.5–6.3	4.7–8.4	13 (n_8)	10.4 (n_8)	17–65 (n_8)
$EI[n_{11}]$	–	4.4–8.0			
$EI[n_{15}]$	1.4–2.6	3.1–5.6	14.4 (n_{17})	9 (n_{17})	–
$EI[n_{6-15}]$	2.0–3.7	2.1–3.8	–	–	–
$EI[n_{11}$ nv]	–	2.4–4.4	0.43 (n_{17} nv)	0.3 (n_{17} nv)	7.2 (n_8 nv)

AMTD
1, 321–374, 2008

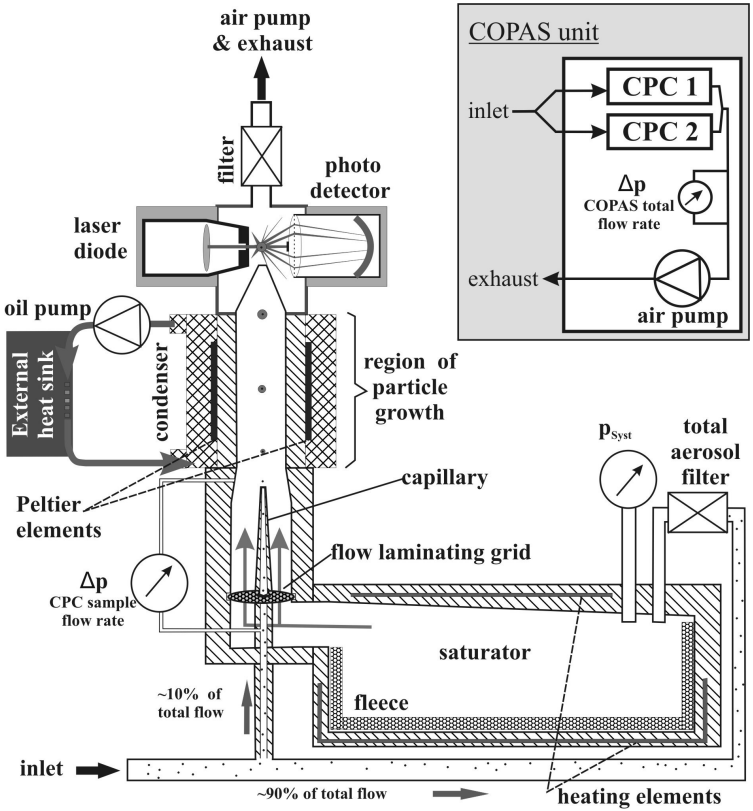

Fig. 1. Flow scheme of a COPAS CPC channel. Two of these counter channels are implemented in one COPAS instrument unit. Two COPAS units (with two CPC channels each) are mounted at different locations on the M-55 "Geophysica".

AMTD
1, 321–374, 2008

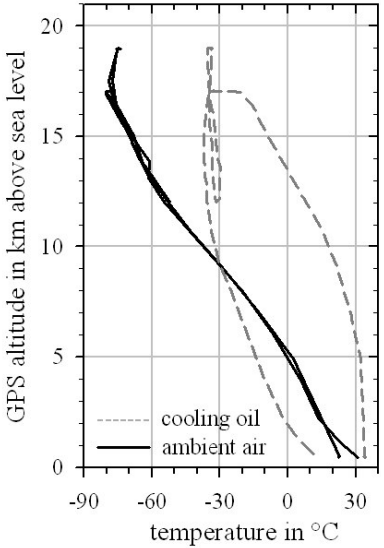

Fig. 2. Vertical ambient temperature profile and the recorded temperature of the cooling oil circuit during a flight (12. February 2005, longitude: 41°–51° west; latitude: 17°–21° south) in tropical regions (State of São Paolo, Brazil).

AMTD
1, 321–374, 2008

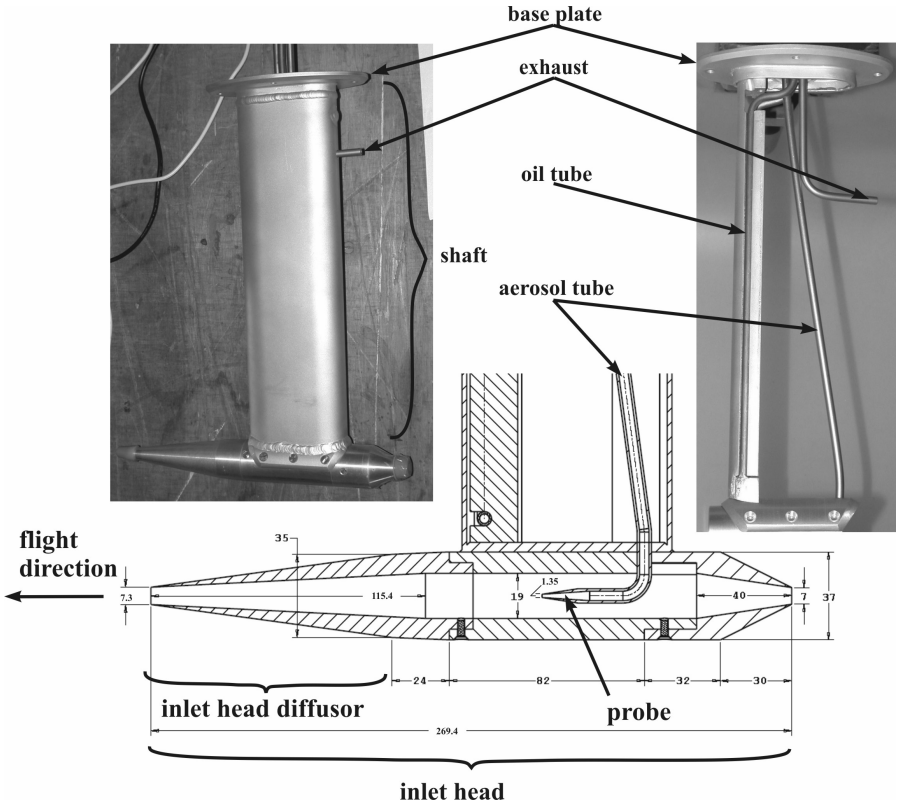

Fig. 3. The COPAS aerosol inlet for measurements on-board the Russian high altitude research aircraft M-55 "Geophysica". The inlet head consists of a diffuser-type entrance with sharp inlet lips. Inside the head, the so-called probe is implemented, also equipped with a diffuser-type inlet with sharp lips. The inlet shaft includes the aerosol intake and exhaust lines as well as the heat exchanger pipes for the silicone oil coolant circuit (Dimensions in millimeter).

AMTD
1, 321–374, 2008

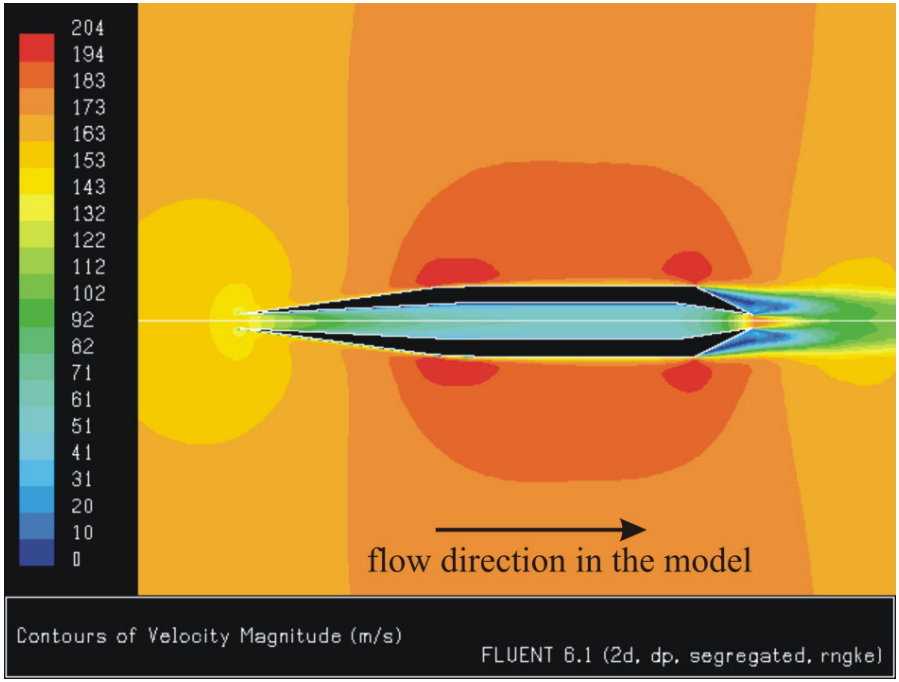

Fig. 4. Air velocity contour plot for the COPAS-inlet from FLUENT CFD calculations. For the model calculation, a free flow velocity of 170 m s^{-1} and an absolute ambient pressure of 50 hPa as well as compressible conditions are assumed.

CC BY

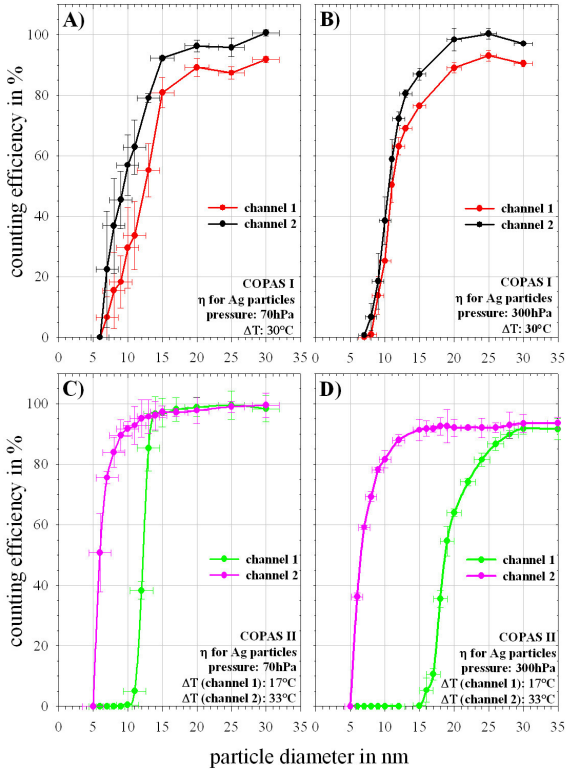

Fig. 5. Results of the experimental COPAS CPC cut-off characterizations compared to an Aerosol Electrometer (AE) at two different system pressures, 70 hPa and 300 hPa. Graphs **(A)** and **(B)** show the counting efficiency curves of COPAS-I, channel 1 (red) and channel 2 (black) operating with a common ΔT of 30°C. The mounted (but not heated) heating line at the aerosol tube of channel 1 and the associated additional particle losses explain the observed differences between the curves. Graphs **(C)** and **(D)** show the result of COPAS-II channel 1 (green) and channel 2 (pink) operated with different ΔT.

AMTD
1, 321–374, 2008

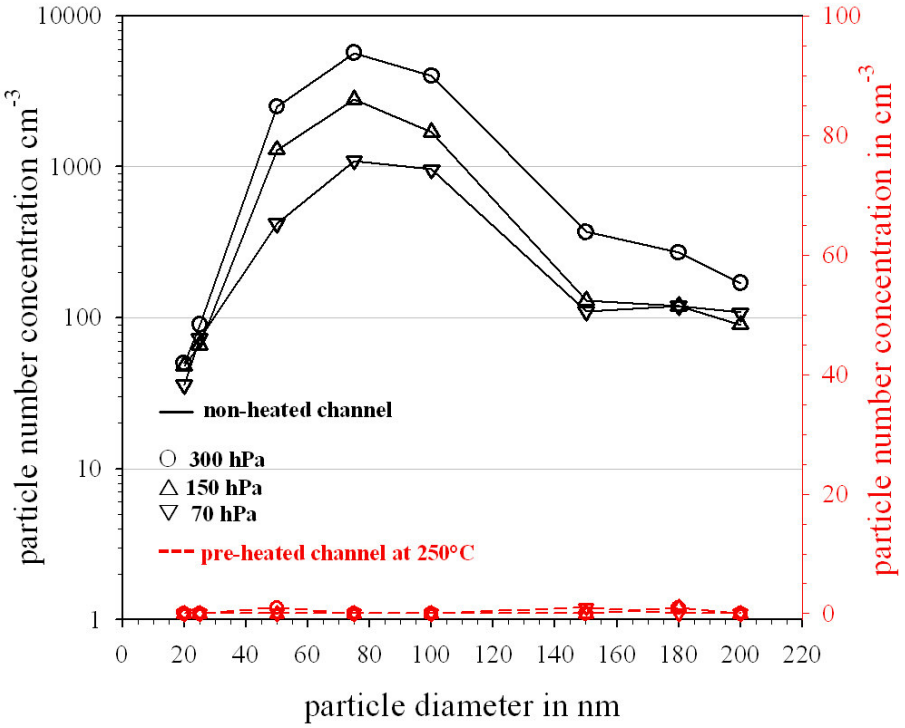

Fig. 6. Result of the experimental aerosol heating line characterization with pure H_2SO_4-H_2O aerosol at a pre-heating temperature of 250˚C for three operating pressures: 70 hPa, 150 hPa, and 300 hPa. The comparison was made between the pre-heated (red) and the non-heated (black) channel of COPAS-I. Note the different scales of the ordinates.

AMTD
1, 321–374, 2008

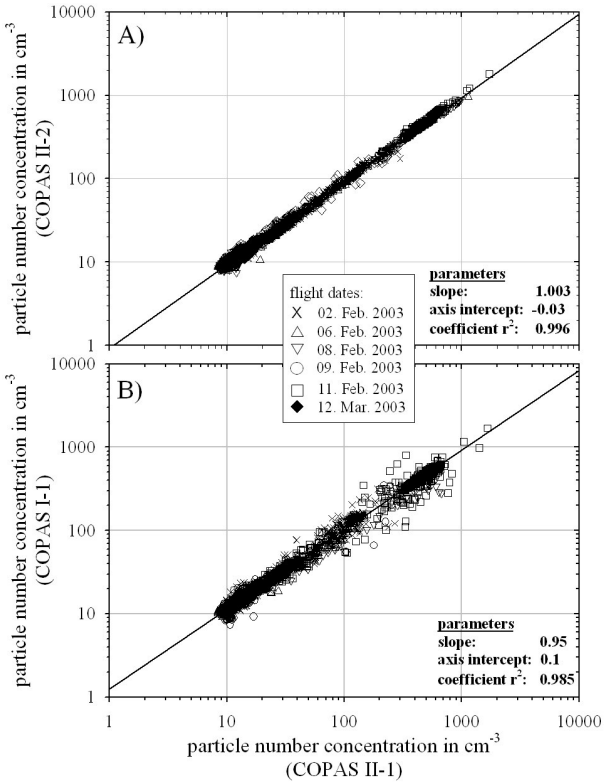

Fig. 7. Correlation of COPAS ambient particle number density measurements (15 s running averaged) from six flights in the arctic lower stratosphere when both COPAS instruments were operated with butanol as well as the same ΔT and therefore identical cut-offs. **(A)** COPAS-II inter-comparison between two channels of the same instrument with a correlation coefficient of 0.996. **(B)** Cross-comparison between one channel of COPAS-I and one channel of COPAS-II with a correlation coefficient of 0.985 (adapted from Curtius et al., 2005).

CC BY

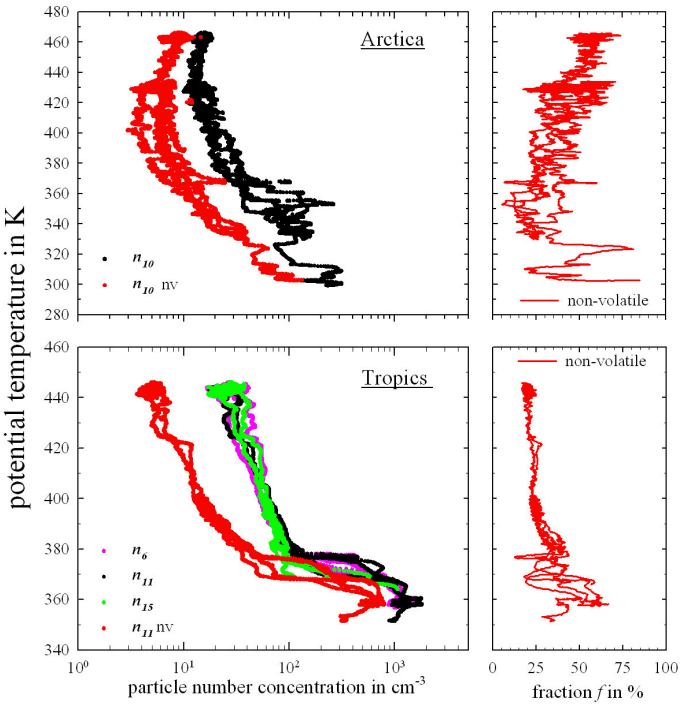

Fig. 8. Vertical profiles of particle number concentration (left) and the vertical distribution of the refractory aerosol fraction (right) measured by COPAS at two different measurement locations. Data are shown as 15-second running averaged versus potential temperature as the vertical coordinate. Upper panel: Flight example from 02 February 2003 (longitude: 10°–30° east; latitude: 68°–76° north) during the polar mission EUPLEX. COPAS working fluid: butanol. Lower panel: Flight example from 12 February 2005 (longitude: 41°–51° west; latitude: 17°–21° south) during the tropical mission TROCCINOX. COPAS working fluid: FC-43.

AMTD
1, 321–374, 2008

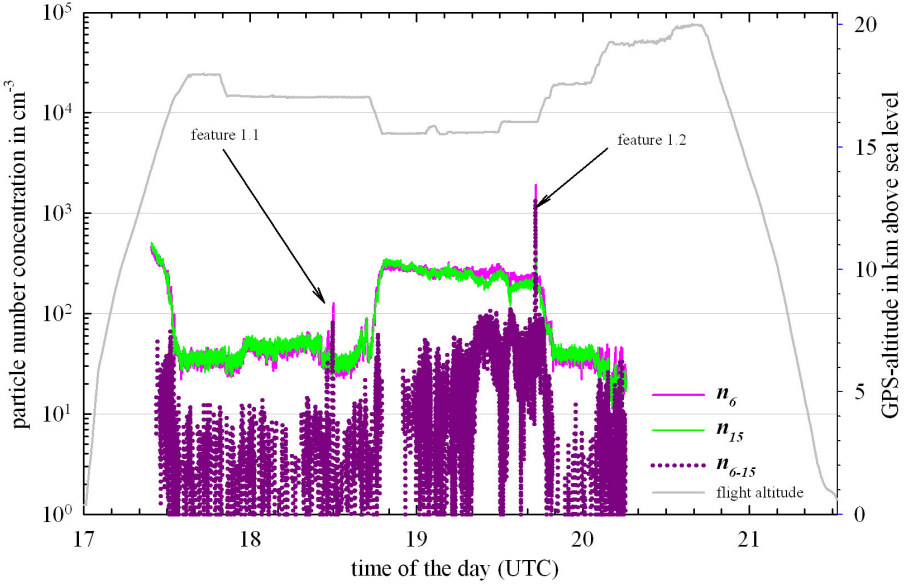

Fig. 9. Time series of COPAS measurements during the flight on 5 February 2005 (longitude: 48°–54° west; latitude: 19°–22° south). Displayed are the measured (1 Hz) ambient particle number concentration n_6 (pink) and n_{15} (green) of COPAS-II as well as the GPS-altitude during the flight (grey line). Two observations of enhanced particle number concentrations are denoted as feature 1.1 and feature 1.2. Additionally, the time series of the ultra-fine particle number concentration difference between n_6 and n_{15} (n_{6-15}) (purple dots) is shown, corrections for coincidence and for particle losses inside the sample lines have been applied.

AMTD
1, 321–374, 2008

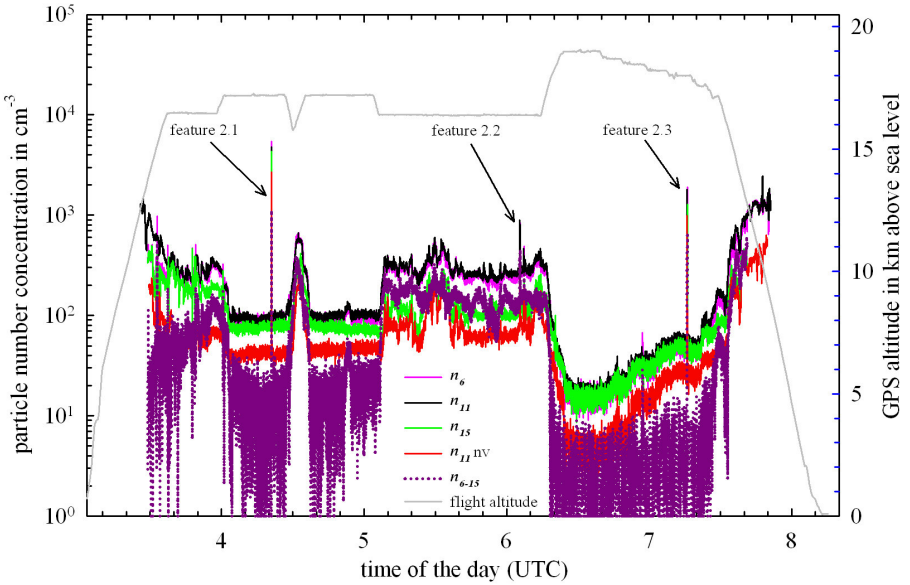

Fig. 10. Time series of COPAS measurements during the flight on 25 November 2005 (longitude: 127°–132° east; latitude: 9°–13° south). Displayed are the measured particle number concentration n_6 (pink), n_{11} (black), and n_{15} (green) as well as n_{10} nv (red) and n_{6-15} (purple dots), corrections for coincidence and for particle losses inside the sample lines have been applied. The GPS-altitude during the flight is indicated (grey). Three observations of enhanced particle number concentrations are denoted as feature 2.1, 2.2 and feature 2.3.

AMTD
1, 321–374, 2008

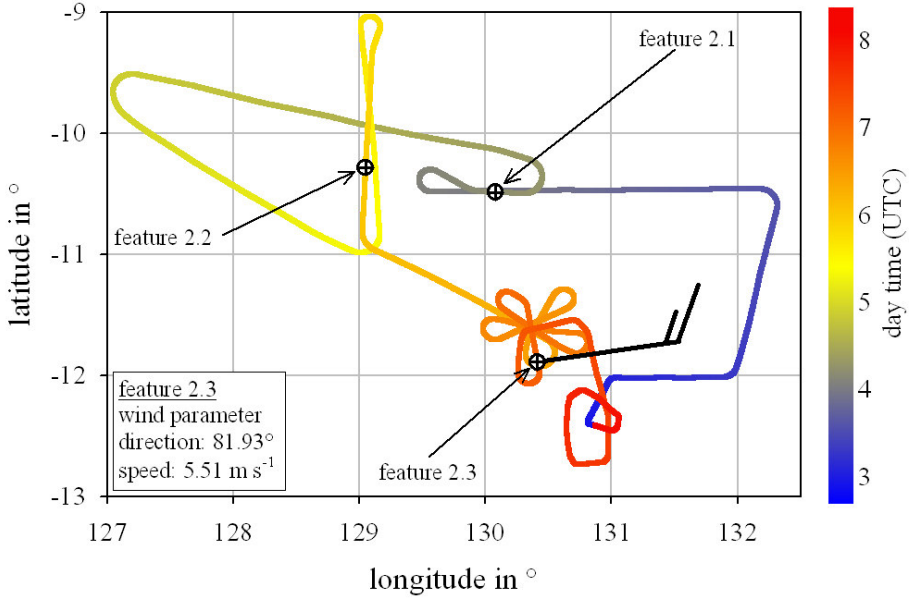

Fig. 11. Projection of the flight path for 25 November 2005. The flight path is shown by the black line, potential plume encounters are labelled as feature 2.1, 2.2, and 2.3 respectively.

AMTD
1, 321–374, 2008